الجامعة الإسلامية العالمية ماليزيا
INTERNATIONAL ISLAMIC UNIVERSITY MALAYSIA
يونيرسيتي إسلام انتارابغسا ملايسيا

INVESTIGATION ON MECHANICAL AND WEAR PROPERTIES OF STRONTIUM MODIFIED ALUMINUM-SILICON ALLOY

BY

ADIBAH AMIR

INTERNATIONAL ISLAMIC UNIVERSITY MALAYSIA

2008

INVESTIGATION ON MECHANICAL AND WEAR PROPERTIES OF STRONTIUM MODIFIED ALUMINUM-SILICON ALLOY

BY

ADIBAH AMIR

A dissertation submitted in partial fulfilment of the requirements for the degree of Master of Science in Manufacturing Engineering

Kulliyyah of Engineering
International Islamic University
Malaysia

JANUARY 2008

ABSTRACT

Wear has deleterious impact on technological use of material and its economy. It was estimated that the direct cost of friction and wear can account nearly 10% of the gross national product (GNP) in many industrial countries, thus research on wear is inevitably vital for developing country like Malaysia. Aluminium-silicon eutectic alloy has been undertaken as a wear testing material in this study due to its best overall balance of properties that are well suited for wear resistance components in the automotive industry. Its low expansion, low density and high resistance to corrosion at ambient temperature characteristics made this alloy an excellent candidate for automotive pistons. Moreover, the addition of small amounts of strontium to the molten aluminium-silicon alloy could produce complete modification of the solidification process. The modification treatment produces remarkable refinement of the eutectic silicon phase and improves the mechanical properties of the alloy. Wear testing has been conducted with a pin-on-disc type wear testing apparatus under lubricant sliding. The test variables were rotational speed, load and sliding distance. In addition to that, attention has been paid to the effects of heat treatment on the strontium modified alloy. The extent of wear damage has been estimated by means of weight loss technique. Possible wear mechanisms of the damaged samples have been investigated with the aid of scanning electron microscope (SEM). From the present investigation, it was found that a considerable improvement in mechanical properties such as an increase in hardness and strength was associated with the resulting structural changes. This lead to an improved tribological performance compared to its unmodified counterparts. Transitional behaviour between fatigue surface, adhesive, abrasive and corrosive wear were exhibited from the worn surfaces. Overall, modified heat treated samples had shown better performance in both mechanical and wear properties.

ملخص البحث

ان التآكل له آثار ضارة على النمو الاقتصادي والتقنـــي. وقـد قـدرت التكاليف المباشرة للاحتكاك، والتآكل بما يقارب 10% من الانتاج القومي العام في عدة دول صناعية، ولهذا الابحاث التي تجرى على التآكل تعتبر ضرورة أساسية وخاصة للدول النامية مثل ماليزيـــــــا.

في هذا البحث قمنا باختيار سبيكة سليكون الألمنيوم اليوتيكتي كمعيار للتآكل لما لها من خصائـص تساعدها على مقاومة التآكل مما يجعلها مناسبة جدا لصناعة السيارات. من هذه الخصائص التمدد المنخفض، الكثافة المنخفضة، والمقاومة العاليـة للتأكسد في درجة حرارة المنطقة المحيطة. هذه الخصائص جعلت سبيكة سليكون الألمنيوم اليوتيكتي مناسبة جدا لصناعة مكابس السيارات. علاوة على هذا، فإن إضافة كميات قليلة من الاسترونتيوم سبيكة سليكون إلى الألمنيوم المصهورة قد تنتج تعديلات كاملة لعملية التصليب. معالجة هذه التعديلات تنتج نقاء استثنائي في السليكون اليوتيكتي. وهذا بالتحديد له أهمية قصوى تفوق التطبيقات والاستخدامات الأخرى لسبك المعادن. اختبار التآكل يمكن أن يجـرى باستخدام عينات اسطوانية تحت زيوت التزليـق. متغيرات(مجاهيل) الاختبار هي: سرعة الدوران، الثقل ومسافـة الانزلاق. بالإضافة إلى هذا، يجب أن نولي اهتماما خاصا لأثار المعالجة الحراريـة على سبيكة الاسترونتيوم المعدلة. ويمكن قياس مدى الضرر الحادث بسبب التآكل باستخدام طريقة الوزن المفقود. آلية التآكل المحتملة للعينات المتضررة يمكن أن تدقق، وتختبر باستخدام مجهر المسح الالكتروني(اس اي ام). يتضح لنا من هذه التجارب التي أُجريت على خصائص التآكل لسبيكة الاسترونتيوم المعدل سليكون الألمنيوم بعد السبك مباشرة أو بعد المعالجه الحرارية أن هناك تطورات وتحسنات كبيرة في الخصائص الميكانيكية، هذه التطورات مرتبطة بالتغير التركيبي الحاصل وبالأخص لتلك العينات التي جرى معالجتها حراريا، وهذا يؤدي إلى تحسن في الأداء الاحتكاكي مقارنة بتلك العينات التي لم تتم معالجتها حراريا. السلوك الانتقالي بين سطح الكلال، المادة اللاصقة، المادة الحاكة (الكاشطة) و التآكل جميعها كانت ظاهرة على السطح المتآكل.

APPROVAL PAGE

I certify that I have supervised and read this study and that in my opinion, it conforms to acceptable standards of scholarly presentation and is fully adequate, in scope and quality as a dissertation for the degree of Master of Science in Manufacturing Engineering.

……..
Md. Mohafizul Haque
Supervisor

I certify that I have read this study and that in my opinion, it conforms to acceptable standards of scholarly presentation and is fully adequate, in scope and quality as a dissertation for the degree of Master of Science in Manufacturing Engineering.

……
Saheb Nouari
Internal Examiner

……
Masjuki Hj. Hassan
External Examiner

This dissertation was submitted to the Department of Manufacturing & Materials Engineering and is accepted as a partial fulfilment of the requirements for the degree of Master of Science in Manufacturing Engineering.

……
AKM Nurul Amin
Head, Department of Manufacturing
& Materials Engineering

This dissertation was submitted to the Kulliyyah of Engineering and is accepted as a partial fulfilment of the requirements for the degree of Master of Science in Manufacturing Engineering.

……
Ahmad Faris Ismail
Dean, Kulliyyah of Engineering

DECLARATION

I hereby declare that this thesis is the result of my own investigations, except where otherwise stated. I also declare that it has not been previously or concurrently submitted as a whole for any other degrees at IIUM or other institutions.

Adibah Amir

Signature: ……. Date:……

INTERNATIONAL ISLAMIC UNIVERSITY MALAYSIA

DECLARATION OF COPYRIGHT AND AFFIRMATION OF FAIR USE OF UNPUBLISHED RESEARCH

INVESTIGATION ON MECHANICAL AND WEAR PROPERTIES OF STRONTIUM MODIFIED ALUMINUM-SILICON ALLOY.

Affirmed by Adibah Amir

……. ……

Signature Date

My praises to the Almighty, with His blessings, this thesis is successfully completed. I dedicated this little gift to my little sunshine, Nuh whom died at the age of two days when I was struggling to bring this work to fruition.

Losing you alongside the triumphs and trials of this work had crushed my heart. In defiance of all laws of medical probability, I wanted you to live, to come home with me. But Allah knows best, He wanted you to come home with Him.

Rest in peace, my dear.

ACKNOWLEDGEMENTS

This quest of knowledge has not only improved my academic work with a master degree, but also in my development as a whole. Therefore, I would like to record my appreciation to these outstanding people for their great contributions.

I wish to express my highest gratitude to my supervisor Prof. Haque. I have benefited tremendous advantages from his scholar expertise and vast experience. Mostly, it was his confidence in me that had inspired me all along the way.

Special thanks goes to the Management Services Division, IIUM for approving my scholarship and study leave application that enable me to pursue this postgraduate study.

I am very thankful to the Dean of Kulliyyah of Engineering for providing all the necessary facilities and equipment, to my boss, Head of Department Manufacturing & Materials Engineering, for the patience he had shown despite the void in the department workforce, to the dedicated technical staff for their efficient assistance despite the late hours, to my dear companions, Sr. Tuti Yasmin Alias for her unflagging support and immeasurable help and Sr. Zuraida Aman Nor Rasid for her continuous involvement beyond the call of academic duty.

Finally, I am indebted, beyond words, in any language to my husband, Azam for his heart warming support.

TABLE OF CONTENTS

LIST OF FIGURES

LIST OF TABLES

LIST OF ABBREVIATIONS

Al	Aluminum	
Cu	Cuprum	
d	diameter	m
E.D.X	Energy Dispersive X-ray	
Fe	Ferum	
H.V	Vickers Hardness	
L	load	N
m	mass	kg or Kg
Mg	Magnesium	
Mn	Manganese	
n	number	
Ni	Nickel	
Pb	Plumbum	
R_A	Roughness average	
rpm	Revolution per minute	
S.E.M	Scanning Electron Microscope	
Si	Silicon	
Sn	Stanum	
Sr	Strontium	
Ti	Titanium	
v or V	volume	m^3
Zn	Zinc	
π	phi	3.142
ρ	density	kg/m^3

CHAPTER 1

INTRODUCTION

1.1 OVERVIEW OF WEAR

To understand wear, it is important to learn first about tribology. The word tribology is derived from the Greek word tribos meaning friction, rub, grind or to wear away (Bushan, 1999). Compact Oxford English Dictionary 2005 defines tribology as the branch of science and technology concerned with surfaces in relative motion, as in bearings. An elaborated definition by Tsujimura and Kikawa in 1998 described tribology as a science and technology concerning two planes in relative motion and interference with each other, and several problems and practical applications. It is noteworthy that the definition refers to practical applications and involves technological viewpoints. It includes the boundary fields between mechanical engineering, physics, chemistry, metallurgy and other disciplines.

Tribology is to control friction, traction and lubrication, and reduce surface damage such as wear, seizure and contact fatigue (Tsujimura and Kikawa, 1998). Whereas wear is a much younger subject, and it was initiated on a largely empirical basis. Scientific studies of wear developed little until the mid twentieth century (Bushan, 1999). Wear is defined as the progressive loss or removal of material from a surface as a result of relative motion between that surface and another (Bayer, 1985). It is closely related to friction and lubrication.

Bayer stated that wear problems can limit the performance of industrial machinery, causing a considerable loss of efficiency, and reducing the intended

lifespan of the equipment. There are varieties of wear mechanisms that include following six principals:

1. Adhesion,
2. Abrasion,
3. Fatigue,
4. Impact by erosion and percussion,
5. Chemical (or corrosive),
6. Electrical-arc-induced wear, etc.

A variety of parameters influence all wear mechanisms, including:

1. Material parameters: composition, grain size, modulus, thermal conductivity, degree of work hardening, hardness, etc.
2. Design parameters: shape, loading, type of motion, roughness, vibration, cycle time, etc.
3. Environmental parameters: temperature, humidity, atmosphere, contamination, etc and
4. Lubrication parameters: type of lubricant, lubricant stability, type of fluid lubrication, etc.

1.2 ECONOMIC IMPACT OF WEAR PROBLEM

Wear has important technologic and economic significance because it changes the shape of the workpiece, tool and die interfaces. Hence, it affects the process, size and quality of the parts produced. The magnitude of wear problem is evident in the countless parts and components that continually have to be repaired or replaced (Bushan, 1999).

According to some analysts, the direct costs of friction and wear can account for nearly 10% of the gross national product (GNP) in many industrial nations (Taylor, 2002). To show the technological impact, friction and wear are estimated to cost the US economy 6% of the gross national product. In a $12 trillion GNP, this translates to over $700 billion per year (Braiman, Cummings and Granick, 2004). Thus, it is understood why researches on wear are very crucial, because the total possible saving is measured not in fractions of a percent but at the important level of several percent of the GNP.

For many years aluminum silicon eutectic alloy (also known as piston alloy) has been used for making piston in automotive industry. In the present study, the piston alloy is modified with strontium and is subjected to heat treatment to improve its mechanical and wear properties. Modification with strontium will produce the desired small well dispersed silicon particles by refining the needle like eutectic silicon phase and eliminating the hard diamond shape primary silicon. With improved fineness and uniform distribution of silicon particles in the structure, the properties of the alloy are accentuated. Furthermore, the full heat treatment of the modified alloy makes the alloy harder and stronger which resists wear damage.

It is hoped the findings from this research can be useful for local automobile spare parts manufacturers to produce piston that can offer higher strength and hardness, higher resistance towards wear, and overall longer life span. In addition to that, manufacturers will be able to offer extended warranty for the said parts or components.

1.3 RESEARCH OBJECTIVES

The present study has been carried out to achieve the following objectives:

1. To investigate the mechanical and wear properties of LM-6 alloy used in automotive industry by modification with strontium and comparing the performance between the modified and unmodified alloy in the as-cast and heat treated conditions.
2. To develop improved materials in terms of mechanical and wear properties with the traditional materials used as a bench mark to show whether any improvement has been achieved or not in the new material.
3. To observe and identify wear mechanisms under lubricant sliding condition that has been used in practical devices that are usually complex and resist simple categorization.
4. To perform experiment on pin-on-disk type wear testing apparatus to determine the sliding wear behavior of material pairs and its correlation by using following three variables:
    a) Increasing load,
    b) Increasing rotational speed and,
    c) Increasing sliding time/distance.
5. To put forward some useful recommendations and suggestions towards the tribological use of this alloy for local automobile spare parts manufacturers.

Overall, this research has been divided into five chapters. The first chapter is an introductory chapter, the second chapter elaborates at length on the literature review relevant with the subject investigated in this thesis. The third chapter is the detailed methodologies of all the experiments conducted in this study, including related

diagrams and calculations. Chapter four relating results have been combined with discussions chapter. The results that have been presented were critically analyzed and discussed with concrete evaluations. Finally, chapter five includes the conclusions that highlighted the prime objectives have successfully been achieved. Therefore, this study is able to contribute its findings to the local automotive industry and hence, the overall national economy of the country.

CHAPTER 2

LITERATURE SURVEY

2.1 INTRODUCTION

Wear is not a basic material property, but a system response of the material (Bayer, 1995). According to Bushan (1999) wear is not only based on loss of material, but damage due to material displacement on a given body (under microscopic view), with no net change in weight or volume, also constitutes wear. Another definition from Antler (1981) described wear as the loss of material as loose particles from solid surfaces as a result of mechanical action. This includes dimensional changes or roughening due to metal transfer in the absence of loose particle formation, the cracking of brittle noble metal platings with the resultant exposure of base metal substrates, and even mechanically induced metal flow without measurable transfer or loss.

The earliest significant contribution to the study of wear was made by Ragnar Holm in 1938. Starting with a clear concept of surface topography and of plastic deformation, he recognized that two surfaces when brought together touch at asperities and that the area of contact is related to the load divide by the yield pressure of the metal. Further, the first quantitative statement of wear is also an attribution by Holm in 1946. He had showed that volume wear (W) might be directly proportional to sliding distance (s), and to the real area of contact P/H, where P is the load and H is the yield pressure of the metal.

2.2 ADHESIVE WEAR

Adhesive wear is a very serious form of wear characterized by high wear rates and a large unstable friction coefficient. Sliding contacts can rapidly be destroyed by adhesive wear. Particularly metals that are prone to adhesive wear (Stachiowak and Batchelor, 1993). This type of wear occurs when two smooth bodies are slid over each other, whether lubricated or not, and fragments are pulled off one surface and adhere to the other. These fragments may come off the surface on which they are formed and be transferred back to the original surface, or form loose wear particles. Scratches caused by adhesive wear are often irregular and shallow (Rabinowicz, 1995; Bushan, 1999).

It had been observed that many systems operate at widely different rates of adhesive wear. This is called mild and severe adhesive wear, and that the scale of wear may change in a narrow range of load (Archard and Hirst, 1956). Wear transition is also evident in the cases of metallic sliding, especially with poor lubricated or unlubricated pairs. It was found that there are two types of sliding behavior, one involving a high wear coefficient and the removal of large metal wear particles is called severe wear whereas, the other with low wear coefficient and the removal of small oxides wear particles is called mild wear (Rabinowicz, 1995). Figure 2.1 shows that below the transition load with base metals, wear debris is finely divided (10^{-2} to 10^{-4} mm); above it, debris, is largely metallic and coarse (1 to 10^{-1} mm). The transition occurs due to the loss of protective oxide in the case of dry sliding, or from lubrication failure. Metallic surfaces free of oxide films under high vacuum exhibited the most dramatic changes (Antler, 1981).

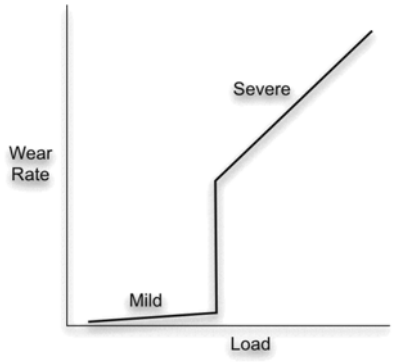

Figure 2.1: Regimes of Wear (Antler, 1981)

It has been found in experiments conducted in vacuum that as the degree of surface contamination is reduced, adhesion between metallic surfaces becomes very large (Bowden and Rowe, 1956). It is evident from Table 2.1 that in all cases the adhesion or the separation force is greater than the contact force. The tendency to adhere does not discriminate between metals on the basis of their mutual solubility or relative atomic size. The greatest adhesion occurs for a combination of like materials, i.e. iron to iron, but many other unlike metals also show quite high adhesions. The ratio of adhesion force to contact force can be very high, about 20 and above in some cases. The bonding process is almost instantaneous and can occur at moderate or low temperature (Buckley, 1981).

Table 2.1
Adhesion force of various metals against iron in vacuum (Buckley,1981)

Metal	Solubility in iron (atomic %)	Adhesion force to iron (mN)
Iron		>4.0
Cobalt	35	1.2
Nickel	9.5	1.6
Copper	< 0.25	1.3
Silver	0.13	0.6
Gold	< 1.5	0.5
Platinum	20	1.0
Aluminum	22	2.5
Lead	Insoluble	1.4
Tantalum	0.2	2.3

Numerous tests on a wide variety of metal combinations have shown that when there is strong adhesion, transfer of the weaker metal to the stronger occurs as illustrated schematically in Figure 2.2.

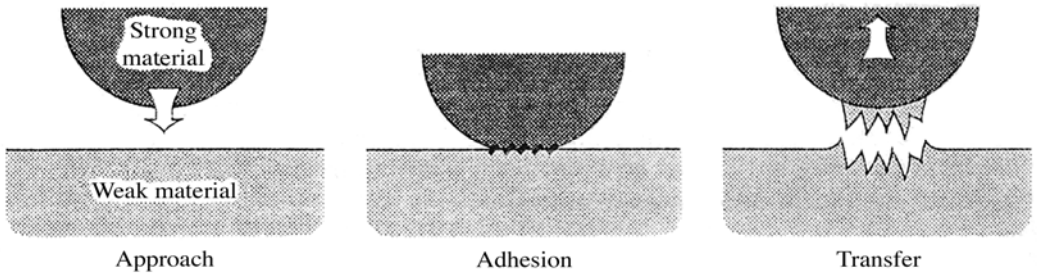

Figure 2.2: Process of metal transfer due to adhesion **(**Stachowiak and Batchelor, 1993).

Electron transfer between contacting surfaces can explain the strong adhesion observed between metals. Numerous free electrons are present in metals and on contact electrons may be exchanged between the two solids to establish bonding. All

metals show a strong tendency to adhere on contact with another solid but there are significant differences between particular elements.

It has been found that asperities with large slope angles or sharper asperities tend to loose material to asperities with small slope angles (Kayaba and Kato, 1979). Material properties have a strong influence on asperity deformation and the severity of adhesive wear. Experiments conducted on model asperities revealed that the contacting asperities of brittle materials tend to break away cleanly with little deformation and produce fewer wear particles compared to ductile materials. It appears that ductility has an undesirable effect of accentuating adhesive wear (Bowden and Tabor, 1964). Figure 2.3 shows the mechanism of shearing and cracking to form a wear particle in the adhesive contact between asperities.

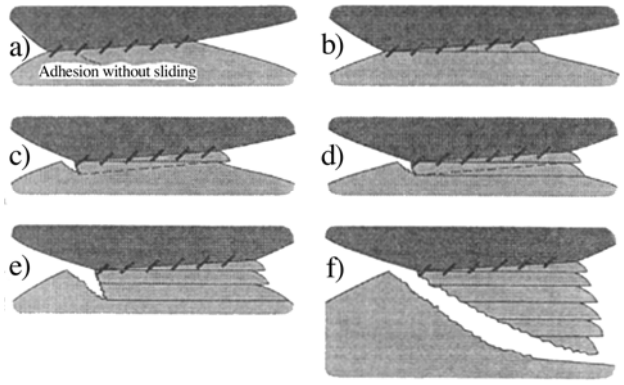

Figure 2.3: Schematic diagram of the formation of an adhesive transfer particle (Kayaba and Kato, 1979)

The particle of metal detached from one of the asperities remains attached to the other surface depending on conditions it may subsequently be removed by further asperity contact to form a true wear part or it will remain on the surface to form a

transfer film. Figure 2.4 shows although in the contact between asperities do not produce wear particles there may still be extensive plastic deformation.

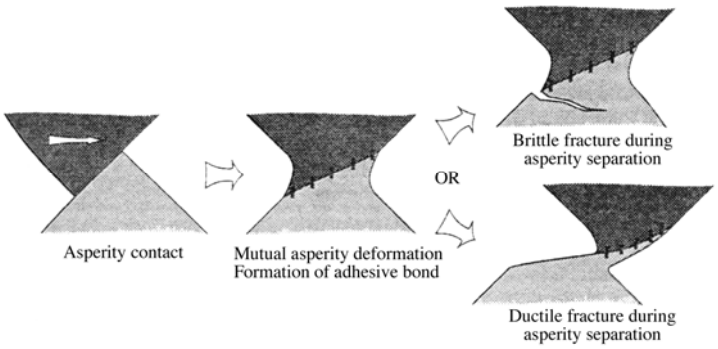

Figure 2.4: Alternative model of deformation in adhesive asperity contact (Vingsbo, 1979)

The mechanism of groove formation involves ploughing of the softer substrate material by work hardened transfer particles (Konivopoulus, Saka and Suh, 1985). The ploughing is a very inefficient form of cutting which can lead to crack formation on the worn surface as a result of high tensile stresses. The mechanism of ploughing by transfer particles is illustrated in Figure 2.5.

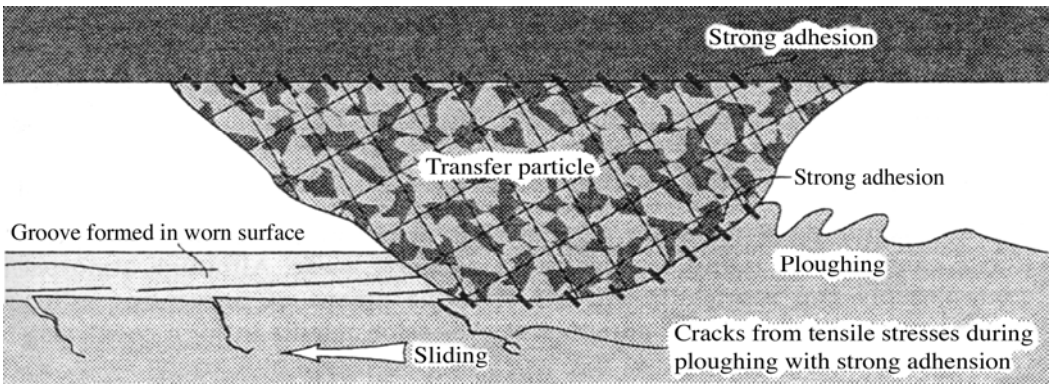

Figure 2.5: Mechanism of groove formation on worn surfaces by work hardened transfer particles (Stachiowak and Batchelor, 1993)

The formation of such coarse grooves on worn surfaces is frequently observed when adhesive wear occurs. These grooves are usually formed on the sliding member with larger track area, e.g. on the disc or ring in pin on disc/ring machines. Most of the frictional resistance in metallic contacts sustaining adhesive wear can be accounted for by the ploughing of a few hardened transfer particles in the softer substrate metal (Konivopoulus et al., 1985).

2.3 ABRASIVE WEAR

Abrasive wear is the loss of material by the passage of hard particles over a surface (Stachiowak and Batchelor, 1993). Abrasive wear occurs when asperities of rough, hard surface or hard particles slide on a softer surface and damage the interface by plastic deformation or fracture (Bushan, 1999). It usually will plough a series of grooves in it. The materials from the grooves is displaced in the form of wear particles, generally loose ones. Abrasive particles tend to produce a sharp, deep scratch (Rabinowicz, 1995). Bayer added that abrasive wear can also occurs when a hard protuberance on the surface of a material or a hard loose particle trapped between surfaces plastically deforms or cuts a surface as a result of motion.

In the case of ductile materials with high fracture toughness (metals and alloys), hard asperities or hard particles result in the plastic flow of the softer material. Most metallic and ceramic surfaces during sliding show clear evidence of plastic flow. Contacting asperities of metals deform plastically even at the lightest loads. In the case of brittle materials with low fracture toughness, wear occurs by brittle fracture. Brittle fracture is favored by high loads acting on each grit, sharp edges on the grit, as well as brittleness of the substrate. When grits move successively across the surface, the accumulation of cracks can result in the release of large quantities of material. In

these cases, the worn zone consists of significant cracking (Bushan, 1999). There are two general situations for abrasive wear, as shown in Figure 2.6.

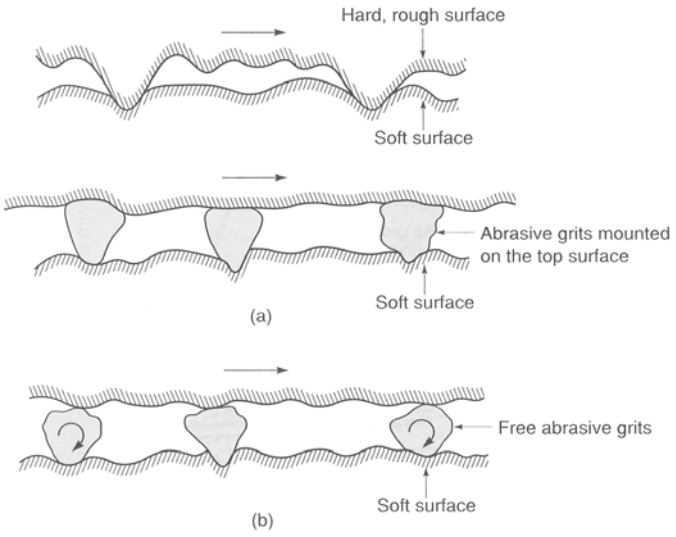

Figure 2.6: Schematic of (a) a rough, hard surface mounted with abrasive grits sliding on a softer surface, (b) free abrasive grits caught between surfaces with at least one surfaces softer than the abrasive grits (Bushan, 1999)

In the case of two-body abrasion (Figure 2.6(a)), the hard surface is the harder of two rubbing surfaces. Whereas in the case of three-body abrasion (Figure 2.6(b)), the hard surface is a third body, generally a small particle of abrasive, caught between the two other surfaces and sufficiently harder that it is able to abrade either one or both of the mating surfaces. In most abrasive wear situations, scratching of mostly the softer surface is observed as a series of grooves parallel to the direction of sliding (ploughing).

During wear, some blunting of the hard asperities or abrasive particles occur, thus reducing the wear rate. Inversely, a brittle abrasive particle can fracture, which

would result in resharpening of the edges of the particle and an increase in wear rate (Rabinowicz, 1995). This is illustrated in Figure 2.7.

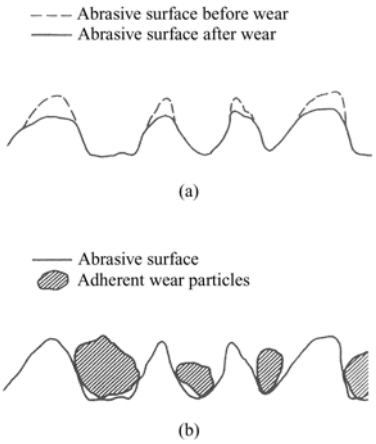

Figure 2.7: Hypothetical appearance of abrasive surface before and after wear (a) showed blunting (b) clogged by wear debris (Rabinowicz, 1995)

A decrease in the wear rate as a function of sliding distance is believed to occur as a result of blunting of the abrasive surfaces in two bodies wear or abrasive particles in three bodies wear, Figure 2.7(a). In addition, clogging of the abrasive surface by abraded debris occurs during wear, Figure 2.7(b). If at any instance, wear debris is larger than abrasive particles, it may leave the material being abraded above the level of the abrasive grains and result in no additional wear. It was noted that abrasive action cease much more rapidly in wear with fine grades of abrasive paper than with coarse grades.

Bushan (1999) had analyzed that material removal from a surface via plastic deformation during abrasion can occur by several deformation modes that include ploughing, wedge formation and cutting. Much of this more complex view of abrasive wear is relatively new, since, like all forms of wear, the mechanisms of abrasive wear

are hidden from view by the materials themselves. Two basic mechanisms were revealed; a cutting mechanism and a wedge build up mechanism with flake like debris, called ploughing (Kayaba, 1984).

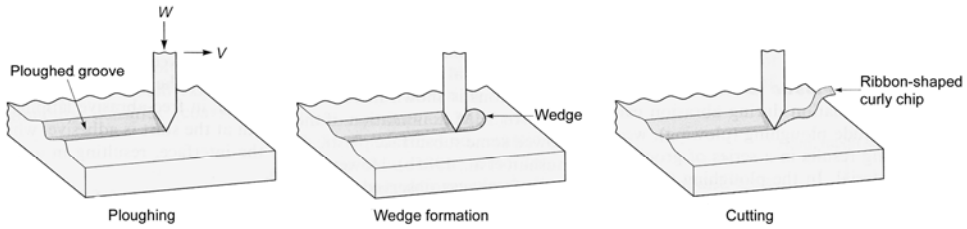

Figure 2.8: Schematic of abrasive wear processes as a result of plastic deformation by three deformation modes; (a) ploughing, (b) wedge formation and (c) cutting (Bushan, 1999)

Ploughing results in a series of grooves as a result of the plastic flow of the softer material. In the ploughing or ridge formation process, material is displaced from a groove to the sides without removal of material. When ploughing occurs, ridges form along the sides of the ploughed grooves regardless of whether or not wear particles are formed. These ridges become flattened, which eventually fracture after repeated loading and unloading cycles. The ploughing process also causes subsurface plastic deformation and may contribute to the nucleation of surface and subsurface cracks.

In the wedge formation type of abrasive wear, an abrasive tip ploughs a groove and develops a wedge on its front. In this situation, only some of the remaining material shows up as a wedge. In the cutting form of abrasive wear, an abrasive tip with large attack angle ploughs a groove and removes the material in the form of discontinuous or ribbon-shaped debris particles. This process results in generally

significant removal of material and the displaced material relative to the size of the groove is very little.

The geometry of the grit also affects the mechanism of abrasive wear. It has been observed that the grit originating from freshly fractured material has many micro cutting edges than the worn grit that has only rounded edges (Stachiowak and Batchelor, 1993). Beneath the surface of the abraded material, considerable plastic deformation occurs. As a result of this subsurface deformation, strain hardening can take place in the material that usually result in the reduction of abrasive wear.

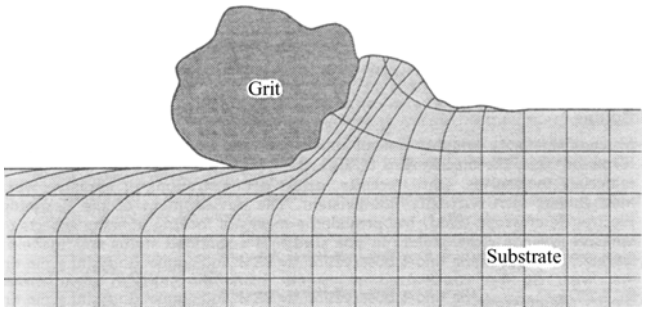

Figure 2.9: Subsurface deformation during passage of a grit (Stachiowak and Batchelor,1993)

To discuss on the abrasivity of particles, a particle or grit is usually defined as abrasive when it can cause rapid or efficient abrasive wear. It has been observed, however, that a limited amount of abrasive wear and damage to a surface still occurs unless the yield stress of the material exceeds that of the abrasive particle. Very slow abrasive wear persists until the hardness of abrasive and worn material are equal.

Another parameter that affects abrasive wear is temperature. It can be divided into;

- The influence of ambient temperature
- The role of temperature rises induced by plastic deformation of the worn material on contact with grits.

The effects caused by these forms of heating are not similar. The influence of elevated ambient temperature on abrasive wear has scarcely been studied. The temperature increase caused by plastic deformation during abrasion is associated with high grit speeds (Wing, 1989). The critical difference between the effects of a temperature rise in the worn metal imposed by high grit speeds and changes in ambient temperature is that the grits remain relatively cool due to the transient nature of abrasion. Contact between a grit and the worn surface would be particularly short in the three-body abrasive wear mode, so that any heat generated in the deformed material would not diffuse into the grit. It is possible then that transient thermal softening occurs only in the deformed material while the grit remains with its virtually unaltered.

2.4 SURFACE FATIGUE WEAR

The term surface fatigue is a technical jargon for surface damage caused by a repeated rolling contact. It refers to the initial damage on a smooth surface and is most often used in the context of rolling bearings. Fatigue requires multiple interactions. In fatigue, a surface experiences repeated stress cycling, leading to cracking. The cracks link and result in the formation of a loose wear particle (Bayer, 1985).

In many lubricated contacts adhesion between the two surfaces is negligible, yet there is still a significant rate of wear. This wear is caused by deformations

sustained by the asperities and surface layers when the asperities of opposing surface make contact. Contacts between asperities accompanied by very high local stresses are repeated a large number of times in the course of sliding or rolling, and wear particles are generated by fatigue propagated cracks, hence the term fatigue wear. Wear under these conditions is determined by the mechanics of crack initiation, crack growth and fracture. Worn surfaces contain very high levels of plastic strain compared to unworn surfaces. This strain and the consequent modification of material's microstructures have a strong effect on the wear process (Stachiowak and Batchelor, 1993).

Surface fatigue wear is observed during repeated sliding or rolling over a track. The repeated loading and unloading cycles to which the materials are exposed may induce the formation of surface or subsurface cracks, which eventually will result in the breakup of the surface with the formation of large fragments, leaving large pits in the surface. Prior to this critical point (which may vary from hundreds to millions of cycles), negligible wear take place, which is in marked contrast to the wear caused by an adhesive or abrasive mechanism, where wear causes a gradual deterioration from the start of running. Therefore, the amount of material removed by fatigue wear is not a useful parameter. Much more relevant is the useful life in terms of the number of revolutions or time before fatigue failure occurs (Bushan, 1999).

Surface fatigue wear is of great practical importance in that it constitutes the main mode of failure of rolling contact elements. This form of wear is closely related to the general phenomenon of fatigue of materials in that there is a characteristic interrelation between the stresses in the contacting materials and the number of cycles required to produce fracture. Adhesive and abrasive wear are operative during direct physical contact between two surfaces moving relative to each other. If the two surfaces are separated by a fluid film (with abrasive excluded), these wear

mechanisms do not operate. However, in an interface with nonconforming contact, the contact stresses are very high and fatigue mechanism can be operative. In these cases, although direct contact does not occur, the mating surfaces experience large stresses, transmitted through the lubricating film during the rolling motion (Rabinowicz, 1995).

When sliding made contact via asperities, wear can take place by adhesion and abrasion. However, it is conceivable that asperities can make contact without adhering or abrading and can pass each other, leaving one or both asperities plastically deformed from the contact stresses. As the surface and subsurface deformation continues, cracks are nucleated at and below the surface. Once the cracks are present, either from pre-existed voids or by crack nucleation, further loading and deformation causes cracks to extend and propagate. After a critical number of contacts, an asperity fails due to fatigue, producing a wear fragment. In a sliding contact, friction is generally high compared to a rolling contact, and the maximum shear stress occurs at the surface that leads to surface fatigue. This may be the situation in a boundary lubrication system in which one or several monolayers of lubricant or absorbed surface layers at the interface separate the asperities but contact stresses are still experienced by the asperities (Bushan, 1999).

The experimental study of surface fatigue wear is rather difficult. Until spalling occurs, there are few useful observations that can be made, although from metallographic study of the rolling contact material, it was discovered that the crack that initiates spalling is sometimes located at the surface, at other times below the surface (Rabinowicz, 1995).

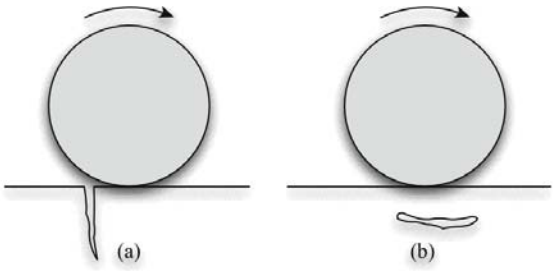

Figure 2.10: Appearance of typical surface fatigue failures in their early stages (a) surface crack (b) subsurface crack (Rabinowicz,1995)

Examination of worn surfaces in cross section reveals intense deformation of the material below the worn surfaces. Under conditions of severe sliding with a coefficient of friction close to unity, material within 0.1 mm of surface shifted in the direction of sliding due to deformation caused by the frictional force. Also, close to the surface the grain structure is drawn out and orientated parallel to the wearing surface. Obviously, under the lower coefficients of friction that prevail in lubricated systems, this surface deformation is less or sometimes absent (Rabinowicz, 1995).

Strains caused by shearing in sliding are present some depth below the surface reaching the extreme values at the surface. The strain levels in a deformed surface layer are shown in Figure 2.11.

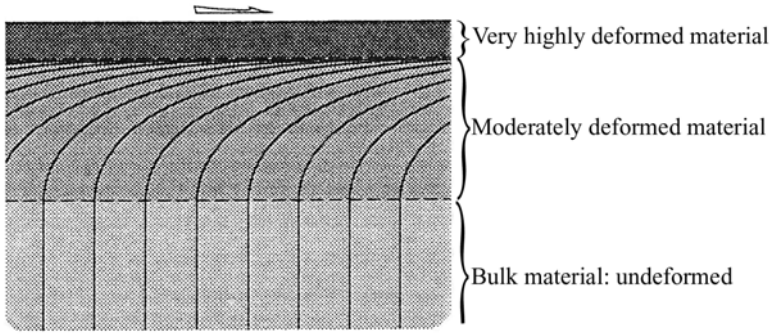

Figure 2.11: Strain levels in a deformed surface (Rigney and Hirth, 1979)

The strain induced by sliding eventually breaks down the original grain structure at the surface to form dislocation cells. These cell can be described as submicron regions, relatively free from dislocation. Materials vary greatly in their tendency to form dislocation cells that according to general metallurgical theory, depends on stacking fault energy, i.e. high stacking fault energy promotes cell formation. Aluminum in this case, have a high stacking fault energy and therefore readily form dislocation cells. At the interface, the cells are elongated in the direction of sliding and are relatively thin resembling layers of flat tiles (Stachiowak and Batchelor, 1993).

The high energy cell boundaries are probable regions for void formation and crack nucleation. The formation of a wear particle can be initiated at the cell walls that are orientated perpendicular to the direction of sliding since the crack can propagate along the cell boundary. Alternatively, the crack can be initiated at a weak point below the surface and subsequently propagate to the surface resulting in the release of a wear particle. Plastic deformations of the surface layer under sliding was simulated by moving a hard blunt wedge against a soft flat surface. It was found that during the process materials piles up in front of the moving wedge without detaching from the surface. During repetitive sliding, the piled up materials does not move with the wedge and instead, the wedge passes continuously through the protuberance of deformed surface (Challen, McLean and Oxley, 1984).

Figure 2.12 shows mechanism of surface crack initiated fatigue wear. A primary crack originates at the surface at some weak point and propagates downward along weak planes such as slip plans or dislocation cell boundaries. A secondary crack can develop from the primary or alternatively, the primary crack can connect with an

existing subsurface crack. When the developing crack reaches the surface again a wear particle is released.

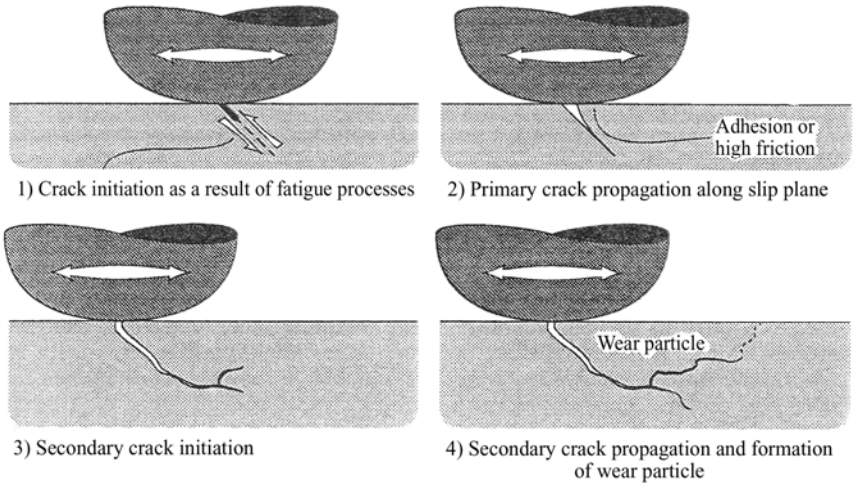

Figure 2.12: Schematic illustrations of the process of surface crack initiation and propagation (Stachiowak and Batchelor, 1993)

Such interaction between different forms of wear happens when an adhesive wear fragment forms because the surface is weakened by fatigue. The fragment abrades the surface and through several deformation cycles, produces a larger fatigue wear particle, or it is swept from the contact and stops the wear. Transfer films are layers generated in a sliding contact by the deposition of wear debris on the surface, frequently they reduce wear type of motion, relative area of one surface to the other and environmental conditions influence transfer film formation. Lubrication influences surface energies, depending on the amount and strength or hardness of the lubricant (Bayer, 1995).

2.5 CORROSIVE WEAR

The fundamental cause of this form of wear is a chemical reaction between the worn material and a corroding medium, which can be either a chemical reagent, or reactive lubricant. Corrosive wear is a general term relating to any form of wear dependent on a chemical or corrosive process (Stachiowak and Batchelor, 1993). The surface chemical reactions which are beneficial in preventing adhesive wear, will, if unchecked, lead to a considerable loss of the underlying material. If a material is corroded to produce a film on its surface while it is simultaneously subjected to a sliding contact then one of the four processes may occur (Rengstorff, Miyoshi and Buckley, 1986);

- A durable lubricating film which inhibits both corrosion and wear may be formed
- A weak film which has a short life time under sliding contact may be produced and a high rate of wear may occur due to regular formation and destruction of the films.
- The protective surface films may be worn (by pitting) and a galvanic coupling between the remaining films and the underlying substrate may result in rapid corrosion of the worn area on the surface
- The corrosive and wear processes may act independently to cause a material loss which is simply the sum of these two processes added together

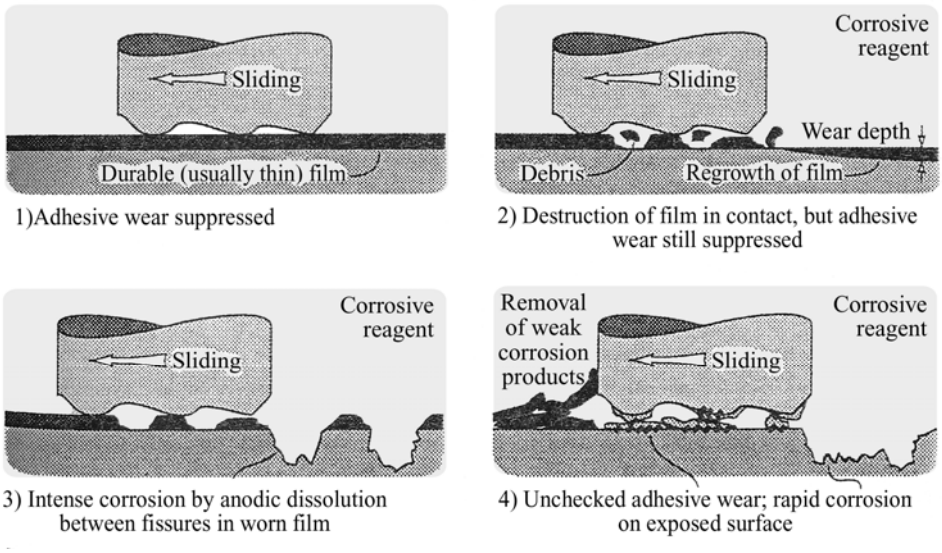

Figure 2.13: Models of interaction between a corrosive agent and a worn surface (Stachiowak and Batchelor, 1993)

The first process is dominated by the formation of durable lubricating films. If such films prevail then the worn contacts are well lubricated and corrosive wear does not occur. Unfortunately, very few corrosion product films are durable so that this category of film formation is rarely seen in practice. The second process is related to the formation of a sacrificial or short lifetime corrosion product film under sliding contacts. This is the most common form of corrosive wear since most corrosive films consist of brittle oxides or other ionic compounds. The third process relates to wear in highly corrosive media while the fourth process is effectively limited to extremely corrosive media where corrosion products are very weak and are probably soluble in the liquid media. It is very unlikely that wear and corrosion, if occurring in the same system, can proceed entirely independent since the heat and mechanical agitation of a sliding contact would almost inevitably accelerate corrosion (Stachiowak and Batchelor, 1993).

The formation and subsequent loss of sacrificial or short lifetime corrosion films is the most common form of corrosive wear. This form of wear can be modeled as a process of gradual build-up of a surface film followed by a near instantaneous loss of the film after a critical period of time or number of sliding contacts is reached. Since most corrosion films passivate or cease to grow beyond a certain thickness this is a much more rapid material loss than static corrosion alone (Tao, 1969). The process of corrosive wear by repeated removal of passivating films is shown in Figure 2.14.

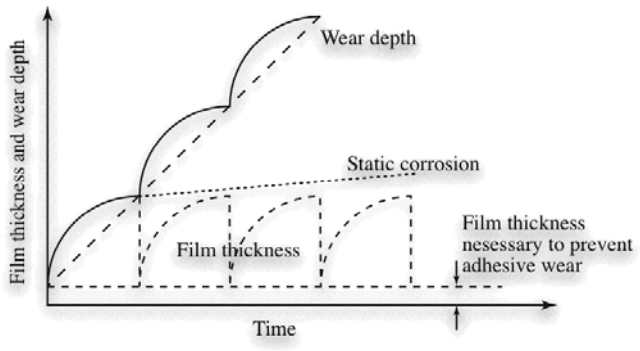

Figure 2.14: Model of corrosive wear by repeated removal of passivating films (Tao, 1969)

The model implies that a smooth worn surface together with corrosion products as wear debris is produced during the wear process that is well confirmed in practice. Typical example of corrosive wear can be found in situations when overly reactive additives used in oil are contaminated with water.

Corrosive wear occurs when sliding takes place in a corrosive environment. In the absence of sliding, the products of the corrosion will form a film on the surfaces. This tends to slow down or even arrest the corrosion. However, the sliding action

wears the film away, so the corrosive attack continues (Rabinowicz, 1995). Transition between corrosive and adhesive wear may occur as the corrosivity of a medium is reduced it may become a good lubricant at a certain level of load and sliding speed. However, an excessive reduction of corrosivity or reactivity of a lubricant may result in severe adhesive wear because of the insufficient generation of protective surface films (Stachiowak and Batchelor, 1993). Therefore the composition of lubricants can be optimized to achieve a balance between corrosive and adhesive wear which gives the minimum wear rate, as illustrated in Figure 2.15.

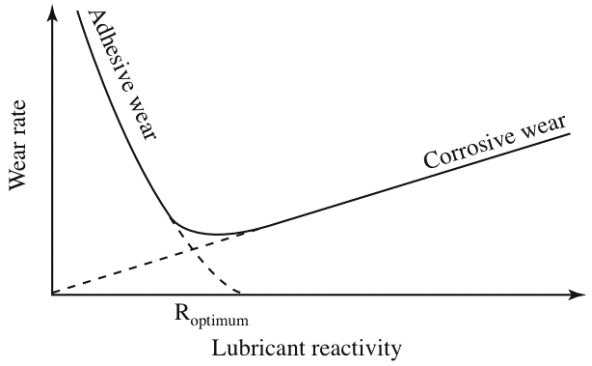

Figure 2.15: Balance between corrosive and adhesive wear (Stachiowak and Batchelor, 1993)

It can be seen from Figure 2.15 that if the lubricant reactivity is too low then adhesive wear dominates which can be severe. On the other hand if the lubricant reactivity is too high then corrosive wear becomes excessive. Thus, there is an optimal lubricant reactivity for particular operating conditions. The transition between sufficient corrosion to generate protective films and adhesive wear is present in most systems. The transition is dependent on load since as the load is increased, more asperities from opposing surface make contact at any given moment so that the

average time between successive contacts for any single asperity is reduced. Consequently, a higher additive or media reactivity is required when load is increased (Stachiowak and Batchelor, 1993).

Similarly, transition between corrosive and abrasive wear may also take place. Abrasion can accelerate corrosion by the repeated removal of passivating films and a very rapid form of material loss may result. The generally accepted model of corrosive-abrasive wear is shown in Figure 2.16. This model is based on cyclic film formation and removal by corrosive and abrasive action respectively.

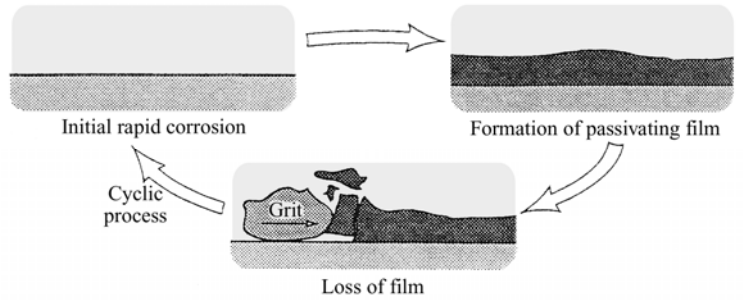

Figure 2.16: Cyclic removal of corrosion product films by abrasion (Stachiowak and Batchelor, 1993)

This mechanism of wear prevails when the rate of mechanical abrasion under dry conditions is less than the corrosion rate without abrasive wear. When mechanical abrasion is more intense, corrosive effects become insignificant. It is probable that when corrosion is slow compared to abrasive wear the grits remove underlying metal with interference from the corrosion film. Resistance of materials under corrosion-abrasion depends on their resistance to corrosion.

2.6 WEAR TESTING

Wear testing has been used to rank wear resistance of materials for the purpose of material selection. One of the most important aspects of wear testing is simulation of actual wear conditions. This requires understanding not only of the intended applications, but also various mechanisms that result in wear. These are the two most common wear classifications because both illustrate the complexity of wear and the need for accurate simulation in wear testing (Bayer, 1985).

- physical mechanisms of material removal and
- operational mechanisms such as sliding wear and material interaction

Wear phenomena can be influenced by load, environment, geometry, motion and counterface. Selection of test geometry when simulating wear conditions. Laboratory sliding contact wear tests employ three general types of contact- line contacts (cylinder on a flat), point contacts (sphere on plane) and conforming contacts (flat on flat). Point or line contact is more sensitive to stress dependant wear mechanisms, because the stress level changes as wear progress. Common wear measure is a geometrical measure, such as mass or weight loss, volume loss or displacement scar width or depth. Indirect measure like time required to wears through a coating or the load required to causes severe wear or a change in surface reflectance. The selection of wear variables to measure wear is often based on convenience, nature of wear specimens, and available techniques (Bayer, 1985).

Wear is related primarily to volume of material removed or displaced, if the tested materials differ in density, weight loss does not provide true ranking. This measure does not account for wear by material displacement, a specimen may gain weight by transfer. When reporting wear data, a description of the wearing system must be supplied because wear is a system response (Bayer, 1985).

The wearing system information includes;

- Apparatus
- Geometry of contact
- Type of motion
- Load
- Speed
- Environmental condition
- Condition of wearing mediums
- Description of materials
- Description of lubricant used

Weighing method is usually the simplest way of detecting wear, since it at once gives the total amount of wear in the form of a single number. This method requires the component to be removed from the sliding mechanism to be examined and cleaned carefully, usually metals by acetone. The limit of resolution of the weighing method is generally around 10^{-4} g. Drawback of this method involved three factors; inability to clean the materials consistently, unpredictable material transfer that occurs at the points when the component is fastened into the sliding mechanism, and the limit of resolution of the typical weighing balance used for wear measurements (Rabinowicz, 1995).

2.7 MODIFICATION WITH STRONTIUM

From the available literature, efforts have been made to comprehend how a small amount of strontium can significantly alter the microstructure of the Al-Si system and consequently enhance it properties. In this section, the reviews were divided into several subsections for ease of understanding.

Because of its commercial importance, study of the modification mechanism has been the subject of intense research efforts dating back to early 1920s when Aladar Pacz had accidentally made this discovery while using an alkali-fluoride treatment in AI-Si melts. The term modification refers to the change in morphology and spacing of the aluminum-silicon eutectic phase induced by the addition of a chemical agent (Shabel, et al., 1995). As the most extensively used modifier, strontium has many advantages;

1. it is permanent, allowing melts to be more effectively degassed, which, in turn provides sounder castings (Shabel et al.).
2. retardation of Mg_2Si precipitation during heat treatment (it can provides the desired small well dispersed silicon particles by refining the primary silicon phase) (Shabel et al.; (Gruzleski et al., 1995).
3. the ability to act as an α – AlFeSi stabilizer if iron is present as an impurity in the alloy, a β- AlfeSi phase which has a deleterious effect on mechanical properties (Gruzleski et al., 1995).
4. it is retained after several remelts without significant loss of modification (alestur.com, 2004).
5. superior fluidity to that of sodium modified (Shabel et al., 1995).
6. less reactive than sodium, so its addition to the melt is safer and easier, plus the attack to the furnace lining is lower (alestur.com, 2004).
7. can effectively to modify eutectic structures over a wide range of freezing rates (alestur.com, 2004).
8. rate of oxidation and loss from the melt is much lower than sodium (Sigworth, 1983).

2.7.1 Effect on Eutectic Temperature and Composition

There is no consensus in the scientific community on the exact mechanism involved. The most popular explanation suggest that modifying addition suppress the growth of silicon crystals within the eutectic, providing a finer distribution of lamellae relative to the growth of the eutectic. Hence, understanding the mechanism by which the eutectic forms and grows is important. During the solidification of aluminum silicon alloys, first the primary dendrites grow. After the dendrites impinge upon each other, the dendrite mobility is restricted. Mass transport to compensate for shrinkage occurs mainly by interdendritic feeding. Interdendritic feeding involves the flow of eutectic liquid. Thus, the origin and growth of the eutectic is of major importance to fluid flow.

Modification of eutectic and hypoeutectic Al-Si allows a transformation of coarse and acicular eutectic silicon to a fine fibrous structure, redistributing the porosity by turning the macroporosity into microporosity (aleastur.com, 2004). Thus by altering the form of the silicon that is a major constituent of these alloys, it plays a significant role in determining the mechanical properties of the alloys.

Lu and Hellawell in 1995 had analyzed that the addition will affects the growth rather the nucleation of the silicon phase. The unmodified structure is characterized by large coarse flakes of silicons that diminish the mechanical properties of the alloy by acting as crack initiation and stress rising sites. The modified structure features a much finer silicon morphology resembling coral or seaweed. The modification results from the absorption of the modifier on the silicon liquid interface and poisons the growth, by blocking the movement of growth steps. This growth poisoning will depresses the temperature for an equivalent growth rate.

The addition of a small amount of modifier to the melt getters the phosphorus, making the nucleation of silicon more difficult. Solidification is therefore suppressed

to lower temperatures where the nucleation rate is large. This leads to a remarkable refinement of microstructure. Thus, it was agreed that Al-Si eutectic could be affected by modification treatment. The difference in growth mechanisms between unmodified and modified Al-Si alloys is manifested in Figure 2.17.

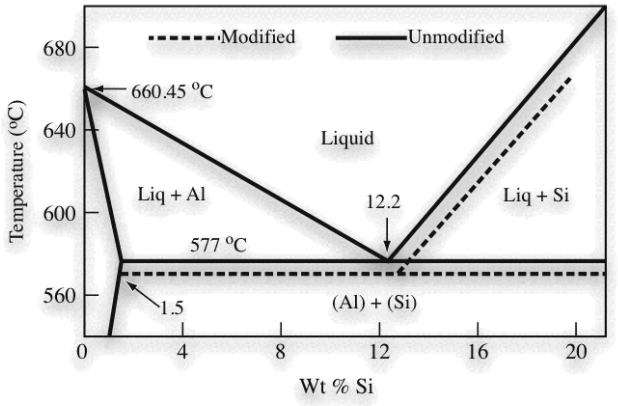

Figure 2.17: Schematic of binary Al-Si phase diagram illustrating the eutectic shift (Emadi and Gruzleski, 1995)

When Al-Si alloy is modified, the eutectic temperature is depressed and the eutectic silicon is changed from coarse plates to fine fibres. While Figure 2.18 shows the greatest depression in the temperature occurs in the unmodified to modified transition**,** the depression of eutectic temperature is only useful to determine if the solidified alloy is modified or not (Gruzleski and Closset, 1990).

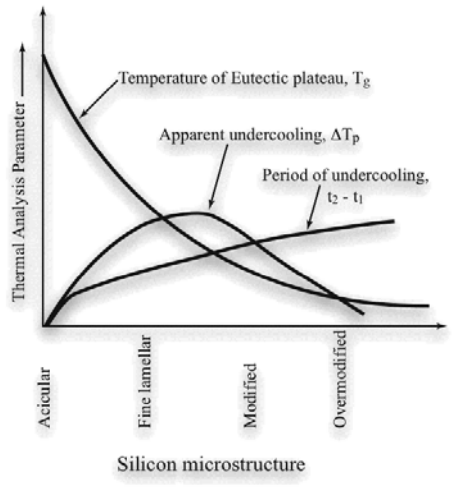

Figure 2.18: Relationship between eutectic structure and eutectic temperature apparent undercooling and period of undercooling (Gruzleski and Closset, 1990)

In an observation made by Haque and Kondic in 1985, the eutectic temperature of the unmodified alloy was recorded at 577º C, which has lowered to 569º C when strontium was introduced into the alloy. Since the modifying elements depress the nucleation temperature, they also lower the growth temperature and change the growth morphology from coarse plates to apparently globular silicon. Figure 2.19 illustrated the cooling curves due to the eutectic solidification of the alloy.

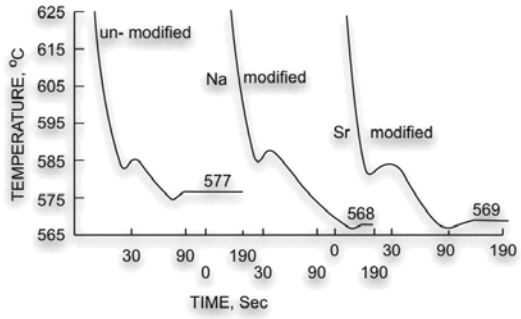

Figure 2.19: Experimental cooling curves for LM6 alloy (Haque and Kondic, 1985)

Figure 2.19 also shows that the pattern of the cooling curves obtained during solidification of LM6 alloy contains various alloying and impurity elements. Each curve shows two arrests, first, the liquidus is caused by the nucleation of primary aluminum solid solution. The number of nuclei depends on the cooling rate and process variables, which later determine the size of the as cast primary dendrites. Once nucleation has started the primary dendrites grow by deposition of further aluminum that cause recalescence. From metallographic examination, it was concluded that highly branched and feathery dendrites resulted from rapid cooling whereas low rates led to more uniform dendrites with fewer secondary arms, the grain size increased in a continuous manner with a decrease in cooling.

Haque and Kondic also mentioned that during growth of the eutectic cells, the liquid between the aluminum dendrites becomes progressively richer in solute elements, since they are rejected by both aluminum and silicon and these form complex phases which at lower temperatures nucleate on the eutectic already present. Growth in these constituents is slow and therefore, a coarse intermetallic network forms throughout the structure to complete the solidification sequence. In the unmodified alloys, the α Al-Fe-Si network is formed and in the modified alloys, a fine acicular β Al-Fe-Si were observed. It was suggested that after solidification of the primary aluminum dendrites, the aluminum-silicon eutectic starts to freeze until the liquid becomes saturated with impurities such as Fe, Mn etc, then the intermetallic constituent forms.

2.7.2 Effects on Microstructure

Varying degrees of modification bring changes from large divorced silicon particles to a fine coupled aluminum-silicon eutectic structure. Some of the critical

microstructural features are grain size, dendritic arm spacing, and silicon morphology in the eutectic phase. Al-Si alloys treated with modifier posses very different microstructures from untreated alloys. Alloys without any modifier contain the silicon phase in the form of plate like particles and a small amount of addition change the silicon morphology to fine globular particles.

This micro structural change is not a sharp reaction, but rather takes place over a range of modifier concentrations. For instance, casting with inadequate amount of modifier leads to a mixed structure. The range of structures observed in modifier treated Al-Si alloys has been divided into six classes in a micro structural standard (Apelian, Sigworth and Whaler, 1984);

1. Fully unmodified structure: In the absence of modifier and with low cooling rate, silicon forms as large plates with sharp sides and ends (acicular)
2. Lamellar structure: When inadequate modifier is added, a lamellar structure can formed
3. Partial modification: When more modifier is used, but still inadequate amounts, the lamellar structure breaks into smaller pieces and forms a partially modified structure
4. Absence of lamellar structure: fine fibrous silicon mixed with a small amount of acicular silicon is found
5. Fibrous silicon structure: fine fibrous silicon is formed without the acicular silicon. This structure is referred to as fully modified structure
6. Very fine structure: Formation of a very fine structure referred to as supermodified.

Haque and Maleque (1998) had observed that the microstructure of modified specimens show that aluminum matrix contains a large amount of rounded silicon with no primary silicon crystal. It also shows one dimensional, rod like growth of silicon rather than two dimensional, plate like growth, as obtained in unmodified alloy.

Study by Haque and Faris in 2005 had shown that when the melt of LM6 is superheated at 750°C, the tensile properties have increased markedly. It means that at lower temperatures, the melts were not modified properly, while at 750°C, the modification was effective. The brittle iron rich phase (β-needle) becomes finer and finer as the superheating temperature is increased, reducing its deleterious effect on the properties of the alloy. Due to structural refinement, the tensile properties of the alloy have enhanced significantly. In binary Al-Si eutectic alloy, cracks usually start around the hard silicon particles, especially those located in the dendrite cell boundaries. These cracks then extend into the soft aluminum and initiate ductile fracture. Thus, strength of the aluminum-silicon binary alloy depends less on its composition than on the distribution and shape of the silicon particles as well as other compounds or networks either primary or eutectic. On the other hand, at the high superheating temperature of 750°C, all phases are refined and well distributed throughout the entire structure. Because of these reasons, the strength and ductility are higher for the alloy superheated at 750°C. Therefore, 750°C can be considered as the optimum superheating temperature for proper modification of Al-Si eutectic alloy with Al-10%Sr temper alloy.

Due to full heat treatment, Haque and Maleque added, both the primary silicon crystals and eutectic needles show some spheroidizing, i.e. the sharp corners have become rounded. It is also noticeable that the modified heat treated alloys have more

uniform and refined structures due to the combined effect of modification and heat treatment.

2.7.2.1 Overmodification

The exact amount of modifier required depends on several parameters such as phosphorus level in the melt and amount of silicon in the alloy. Using a modifier concentration higher than needed has a detrimental effect on the mechanical properties of the alloys because it caused overmodification. Addition of large amounts of modifier (Na >0.02% and Sr>0.1%) causes a change in the morphology of silicon in certain regions of the microstructure (Sigworth, 1983). An intermetallic phase such as Al_4SrSi_2 may appear in the microstructure. This phase is highly faceted and angular and its occurrence decreases the mechanical properties of the cast alloy (Closset and Gruzleski, 1982).

2.7.3 Effect of Holding Time

All of the added modifiers do not necessarily dissolve into the melts. A portion of it can be lost during melt processing because of oxidation or vaporization. Strontium fades when the melt is held for extended periods of time, modifier usually fades with holding time of the melt, this will decreases its effectiveness (Haque, 1983). The main reasons for fading are oxidation and vaporization. Melts with lower surface area to volume ratio will have lower fading rate. Minimizing stirring can also reduce the fading rate because degassing and stirring enhance oxidation or vaporization and this can cause modifier loss into the dross. Vapor pressure of strontium is much lower than that of sodium at typical melt treatment temperature. Therefore vaporization is not an

issue for strontium. Primarily, strontium losses are by oxidation (Sigworth, 1983; Gruzleski and Closset, 1990).

2.7.4 Modification Variables

Several variables can be used to determine the exact microstructure that forms. Among them are;

1. Amount of modifier used
2. Cooling rate during modification
3. Amount of silicon in the alloy
4. Type of modifier used
5. Holding time
6. Degassing and stirring after modification
7. Impurities present in the melt, in particular phosphorus

Phosphorus is the most important impurities. There is always an interaction between modifiers and phosphorus that reduces the extent of modification, but usually, higher levels of modifier can alleviate the problem (Sigworth, 1983). The strontium addition level to be used will depend upon the silicon content of the alloy. Modification of eutectic alloys is more difficult than hypoeutectic ones, requiring higher addition rates. Sand casting requires higher addition rates than permanent mould and die-casting ones (aleastur.com, 2004).

The extent to which strontium becomes capable of refining the eutectic phase of the structure is dependent mainly on its concentration in the molten alloy before commencement of solidification, as well as the growth rate induced. According to Haque and Maleque (1998), the refined structures and properties reach a maximum when strontium concentration is about 0.1%, then tend to decrease with further

strontium additions beyond this level. Since modifying elements depress the nucleation temperature, they also lower the growth temperature and change the growth morphology from coarse plate to apparently globular, which confers better properties.

Study has shown that the degree of undercooling prior to the nucleation of eutectic silicon decreases from 10º C for 12.2 % Si to 6º C for 16% Si and the eutectic arrest temperature which is lowered from the equilibrium value of 577º C by 12.2 %, was raised to 573º C by 16% Si alloy. Therefore the increase of silicon content beyond the eutectic composition of the alloy is accompanied by nucleation at higher temperature that favors primary and coarse plate like eutectic silicon and also makes it difficult to get complete suppression by strontium modification. From metallographic examination, it was observed that the degree of refinement of the eutectic silicon decreased as the addition of silicon was increased beyond the eutectic composition. Clearly there is an upper limit beyond which the appearance of primary silicon crystals is inevitable (Haque and Kondic, 1985).

Strontium is more soluble in solid aluminum than sodium, therefore master alloys with strontium can be produced (Sigworth, 1983). Al-Si-Sr master alloy is the most convenient and economical way of adding strontium to aluminum-silicon eutectic alloys. But there are some limitations of using this metal to affect modification in that it must be added according to certain criteria to obtain satisfactory results (Haque, 1983). The preferred master alloys to add strontium to an Al-Si melt are those with 10%Sr. As the Al-Sr phase diagram shows Figure 2.20, these composition have low melting points and dissolution of the master alloy is relatively simple. Strontium also is known to have higher performance from the addition in form of master alloy compared to sodium (aleastur.com, 2004).

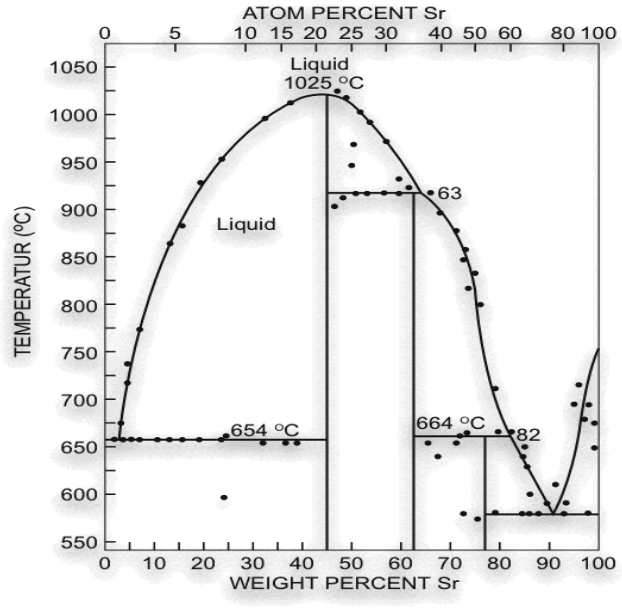

Figure 2.20: Al-Sr phase diagram indicating low melting point for low and high Sr (Sigworth, 1983)

2.7.5 Effect on Mechanical Properties

The addition of strontium secures a substantial increase in the tensile properties of the alloy. This increase may be due to modification of the structure, which changes the shape of the eutectic silicon 'coral' in the aluminum matrix i.e. from a needle like to a rounded morphology (Haque and Maleque, 1998). Dinnis, Otte, Kahle and Taylor (2004) had reported that this modification results in a considerable improvement in mechanical properties, especially elongation.

Haque and Kondic have shown that higher pouring temperature reduces the tensile properties of the alloy, whereas when the melts are poured at comparatively lower temperature, from 720 to 710°C, the results are better. Since higher pouring temperatures result in slower cooling of the casting throughout its freezing range, the degree of undercooling is less and fewer nuclei are available for growth that

eventually lead to the formation of comparatively coarse crystals and hence inferior tensile properties.

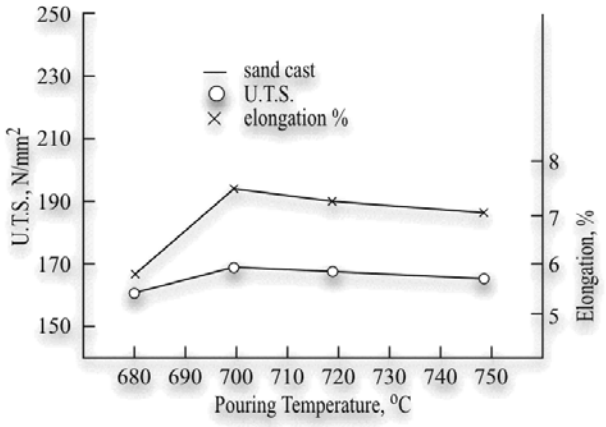

Figure 2.21: Effect of pouring temperature on tensile properties of strontium modified LM6 alloy (Haque and Kondic, 1985)

Mechanical properties of a cast Al-Si alloy depend on several, often interrelated variables such as hydrogen concentration, silicon and magnesium content, heat treatment, cooling rate, impurities, casting soundness, grain refinement and eutectic modification. In order to determine the effect of modification on mechanical properties, these variables must be controlled. In general, major benefit of eutectic modification in the final as-cast product is an improvement in the mechanical properties, most notably elongation. The improvement observed in mechanical properties depends on the effectiveness of modification treatment.

Unfortunately, by a variety of mechanisms, strontium introduces a greater degree of porosity in the final casting (Shabel et al., 1995). It was discovered that strontium had significantly increases the pore volume fraction, pore size and pore number density (Emadi and Gruzleski, 1995). It is well established that porosity forms

through the effects of solidification shrinkage and hydrogen rejection, either individually or in combination. The growth of a pore is determined by a balance between the pressures that promote and oppose pore formation (Dinnis et al., 2004).

CHAPTER 3

EXPERIMENTAL DETAILS

3.1 INTRODUCTION

Various experiments have been carried out before conducting the actual wear tests. All steps are shown in Figure 3.1.

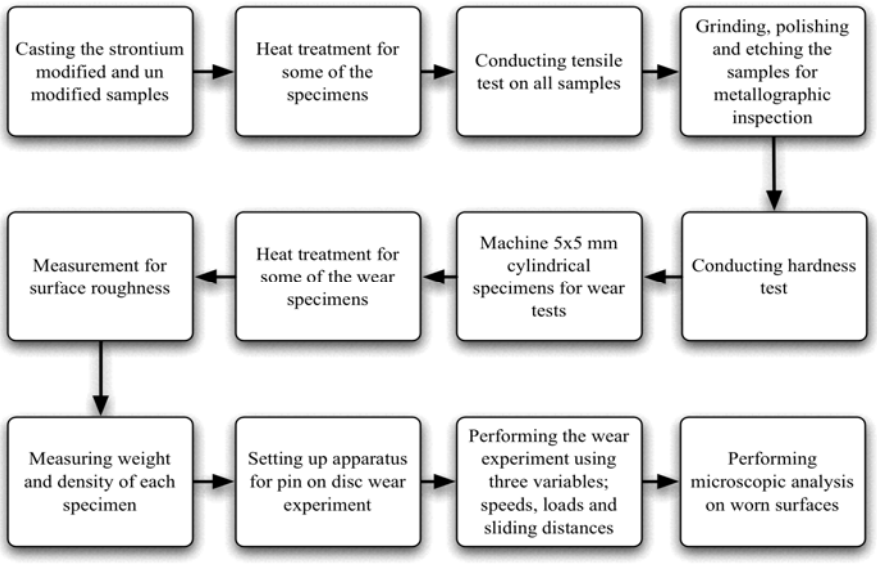

Figure 3.1: Sequence of various stages of experiments

3.2 MOULDING MATERIAL AND MOULD PREPARATION

The moulding mixture consisted of sand grains having sub-angular shape and 10% bentonite clay to which about 6% water was added. They were mixed together in a mulling machine. In order to reduce the effects of variations in moisture content and surface hardness of the mould, the surface hardness and the moisture content of the

green sand aggregate were monitored by using Green surface hardness tester and Speedy moisture tester, respectively.

Figure 3.2 shows the pattern dimensions for making round tensile test bar using green sand as main moulding material. The pattern board contains replica of two tensile test bars (Figure 3.3a), which have been moulded together as shown in Figure 3.3b.

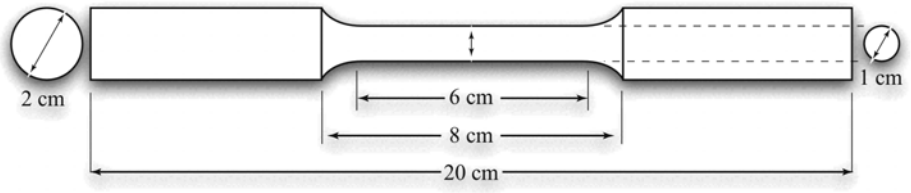

Figure 3.2: Pattern dimensions for round cast to shape and size tensile test bar

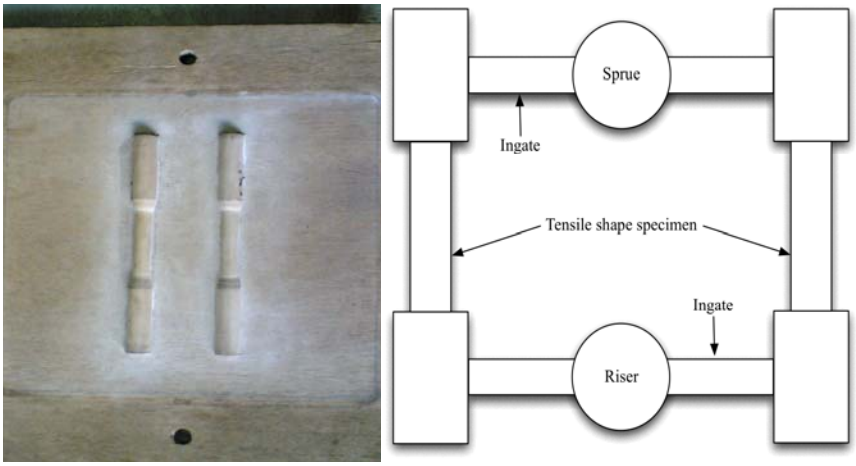

Figure 3.3: Showing (a) wooden pattern and (b) position of the tensile specimens in the mould.

3.3 CHARGE MATERIAL, MELTING AND CASTING

Aluminum-silicon eutectic LM6 type alloy was used in this study. The composition is shown in Table 3.3 below.

Table 3.1
Chemical composition (weight %) of LM6 alloy

Mg	Si	Cu	Fe	Mn	Ni	Sn	Pb	Zn	Ti	Al
0.10	12.20	0.10	0.51	0.29	0.01	0.01	0.01	0.01	0.02	Bal.

Strontium in the form of Al-10% Sr alloy (supplied by Syarikat Limmet, Malaysia), was added to the charge at the beginning of the melt. This temper alloy was cut into small pieces (5-8 mm) and kept at the bottom of the crucible. From the findings of some previous investigators, 0.1% strontium was added to modify the LM-6 alloy in the present study (Haque, 1983). The crucible was then put in an electric furnace (Nabertherm N81/13) for melting and superheating the charge. The superheating temperature of 750^{o} C for the melt was used and the melt was held at these temperatures for about 5 minutes (Haque and Kondic, 1985). The melt was then stirred with a rod coated with bentonite slurry and the dross was skimmed off from the top before pouring. The pouring of the melts was carried out at about 700^{o}-710^{o} C into the green sand moulds (Figure 3.3(a)) in a continuous stream. The tip of the crucible was held just above the pouring cup of the green sand mould and was aligned with the direction of the test bar to avoid any possible turbulence to minimize drossing and hydrogen pick up in the mould. After casting, the mould was shaken to take out the tensile specimens. Figure 3.3(b) shows the tensile specimens with sprue and riser.

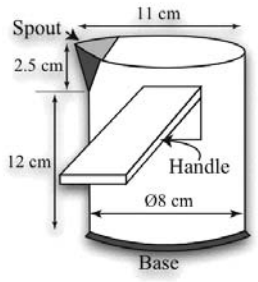

Figure 3.4: Diagram of the metal crucible

3.4 TENSILE TESTING AND HARDNESS MEASUREMENT

Tensile tests were conducted according to ASTM E 8 with Instron Universal Testing Machine Instron 5580 (100 kN). The elongation and the ultimate load for each of the tests were displayed on the machine screen. Further analysis on the ultimate tensile strength and percentage elongation were calculated from these results. The results were averaged from two determinations. The hardness tests were conducted with MicroVickers Hardness Tester MVK-H2 Mitutoyo. The load used is 0.245 N and loading time is about 20 seconds. The final results were averaged from five readings.

3.5 METALLOGRAPHIC TEST

The metallographic specimens were polished according to ASTM Metallography Standard, E3. The specimens were grinded on SiC paper size 400 water cooled, followed by polishing on velvet cloth using diamond suspension 6 µm, then 3 µm and finally on 1 µm. This was necessary to remove the micro-scratches from the specimens. The specimens were then etched in 0.5% aqueous HF acid for about 20 seconds. A Universal microscope (Olympus CK40M) having computerized monitoring system and digital photograph taking arrangement was used for the examination and recording of the representative microstructures.

3.6 MACHINING OF HARDENED STEEL DISK

The disk was machined using ROMI Bridgeport 220V until the required dimensions are achieved as in Figure 3.5. For good surface finish, the disk surface has to undergo facing process under 500 rpm with 0.036 feed per minute. Higher speed causes high vibration that would affect the surface smoothness/roughness.

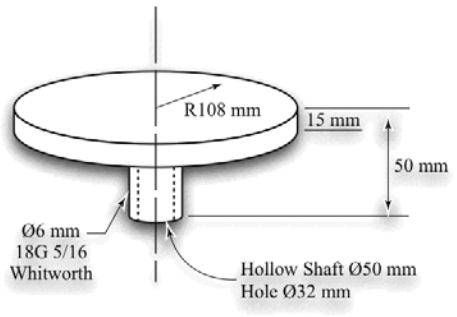

Figure 3.5: Hardened steel disk with dimensions

3.7 MACHINING OF WEAR TEST SPECIMENS

The specimens were brought to undergo turning process with 1400 rpm for surface finish to get about 5 mm diameter with minimum tolerance (0.1 mm) using ROMI Bridgeport 220V. After turning the whole piece, the rod shape sample was cut into 7 mm in height. Each sample was then clamped in the lathe machine for facing process (2000 rpm, feed 0.5 mm/min) to get an actual specimen size of 5mm. The process was then repeated until there were about 80 specimens ready for the wear test experiments.

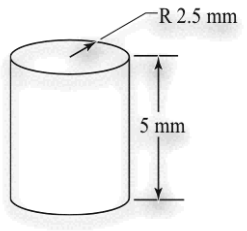

Figure 3.6: Wear test specimen with dimensions

3.8 HEAT TREATMENT

Half of the wear specimens made from unmodified and modified test pieces were taken for full heat-treatment operations. In order to do this, mild steel tray was prepared as shown in Figure 3.7 and it was filled with dry sand up to 5mm. The specimens were then placed on it and put in the electric furnace. The wear specimens was heated in the furnace at 520^{o}C (±5^{o}C) for about 8 hours (Yasmin T. et al.,2004). They were then quenched in hot water at 60^{o}C for about 15 minutes. The wear specimens were then dried and kept at –10^{o}C for overnight in the freezer. The wear specimens were dried and again heated up to 170^{o}C(±2^{o}C) for 8 hours. They were then cooled in the normal room temperature. The same procedure was adopted for tensile test specimens.

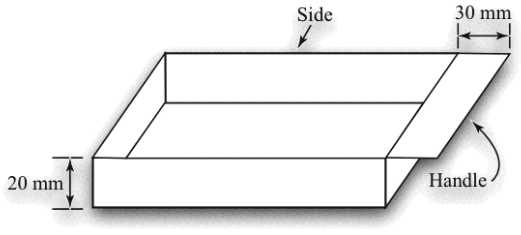

Figure 3.7: Shape and size of heat treatment tray

3.9 SURFACE ROUGHNESS MEASUREMENT

The test was carried using Surface Roughness Profilometer (Surftest SV 500 Mitotoyo). All the wear specimens' surface was wiped with acetone. Each specimen was placed in the three jaw chuck to make it leveled. The stylus was placed approximately at the center of the specimen. The profilometer was operated and the readings were recorded. Average of 3 readings was taken and recorded.

3.10 PIN-ON-DISC TYPE WEAR TESTING APPARATUS

Pin-on-Disc type of testing apparatus has been widely used to study wear properties and to classify the rank of the material. The test was known as a general test that can determine the sliding wear behavior of material pairs and its correlation. It was performed according to ASTM Standard G99 (Eyre, 1991). The parameters for the test include size and shape of the pin, load, speed, sliding distance and counter disk. Details of the drill chuck are shown in Figure 3.8(b), with the schematic diagram of the load, pin disk and direction of rotation.

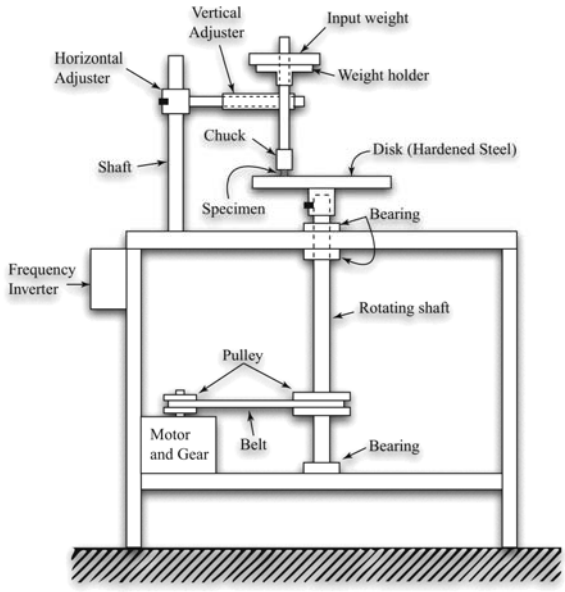

Figure 3.8(a): Schematic diagram of the pin-on-disk type wear testing apparatus.

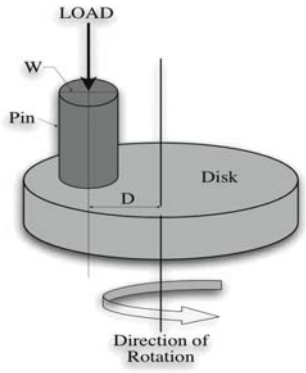

Figure 3.8(b): Diagram for pin-on-disc test

3.10.1 Setting-Up of the Wear Test

The wear specimen and the hardened steel disk were cleaned and dried using cotton dipping with acetone. The mass of each specimen was measured and recorded using 4 decimal point electronic digital balance. SAE 40 engine oil was used as a lubricant during the sliding (AMSOIL, 2003). The specimen was then placed and fitted in the bit slot and tightened by rotating chuck key into the chuck cap. The chuck key rotated

the clamp gear and by rotating the collar, the threaded rod made the collar plate to push the arm and at the same instant tightened the specimens. The specimens were then placed at certain radius of the hardened disk. The radius of the disk in each test was recorded to calculate the sliding distance. Before starting the experiment, the speed was adjusted using the frequency inverter and counter checked by using tachometer. Initial 1.5 kg load was placed on the weight holder. Once the rotation reached the exact frequency that matched with the speed required, the stop-watch was started to record the total time for rotation. When the time was up, the stop button was pushed on the frequency inverter to stop the rotating disk, and the specimen holder was jerked up. The specimen was unclamped from the chuck, and then the lubricant deposit was removed from the specimens and the disk. The final mass of the specimen was recorded, and the worn surfaces were examined using scanning electron microscope to determine the possible wear mechanism.

All tests were performed using following variables;

(a) Three rotational speeds were used as 350, 450 and 550 rpm (keeping both load 2.5 kg and sliding distance 2000 m constant).

(b) Three loads were used as 1.5, 2.5 and 3.5 kg (keeping speed 450 rpm and sliding distance 2000 m constant).

(c) Three sliding distances were used as 1500, 2000, 2500 m (keeping load 2.5 kg and speed 450 rpm constant).

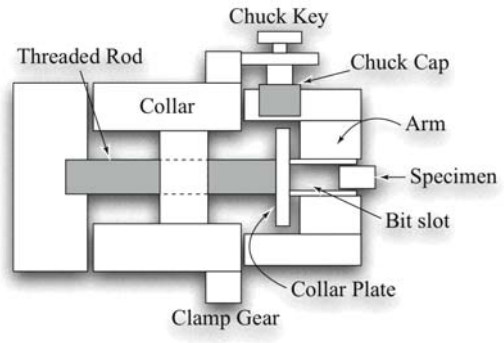

Figure 3.9: Details of specimen holder (drill chuck)

3.10.2 Procedure for Conducting Wear Test

The standard procedures using testing variables were tabulated in Table 3.2. Material loss as a function of wear was determined continuously with different rotational speeds, top loads, and sliding distances. Tests were carried out until all transitions are completed and steady state wear occurs. Worn surface of the specimen were examined using scanning electron microscope. Finally, possible wear mechanisms were suggested.

Table 3.2
Variables in wear testing using pin-on-disk type apparatus

Variables	Values
Load (kg)	1.5, 2.5, 3.5
Rotating Speed (rpm)	350, 450, 550
Sliding Distance (m)	1500, 2000, 2500
Temperature ($^{\circ}$C)	Room Temperature, about 24
Geometry	Circular
Contact Area (m^2)	2.592 x 10-3
Surface finish	Machined surface finish
Atmosphere	Relative Humidity: 70% Atmospheric Pressure: 1 ATM
Materials Used	1) Test Specimens: i. Al-Si eutectic alloy as-cast and heat-treated condition ii. Strontium modified Al-Si eutectic alloy as-cast and heat treated condition 2) Disk Material: Hardened Steel
Counterface –1	1) Al-Si eutectic alloy 2) Strontium modified Al-Si eutectic alloy
Counterface –2	Hardened Steel Disk
Type of lubricant	SAE 40 engine oil

CHAPTER 4

RESULTS & DISCUSSIONS

4.1 INTRODUCTION

In this chapter, results obtained from two phases of experiments such as mechanical tests and wear tests have been presented. At the same time, analysis of the results as well as their comparisons have been made from the results of the other investigators obtained from the literature.

4.2 MECHANICAL TESTING

The first phase of the experiments was carried out to investigate the following:

1. To analyze the microstructural changes due to strontium modification in the modified alloy as compared to the unmodified one, for both in the as-cast and heat treated conditions.
2. To analyze the improvement caused by the addition of strontium on mechanical properties, namely hardness, strength and elongation for modified Al-Si alloy as compared to the unmodified one, both in the as-cast and heat treated conditions.

4.2.1 Effects of Modification on the Silicon Morphology

Microstructures of unmodified and modified LM6 alloy for as-cast condition are shown in Figure 4.1(a) and (b).

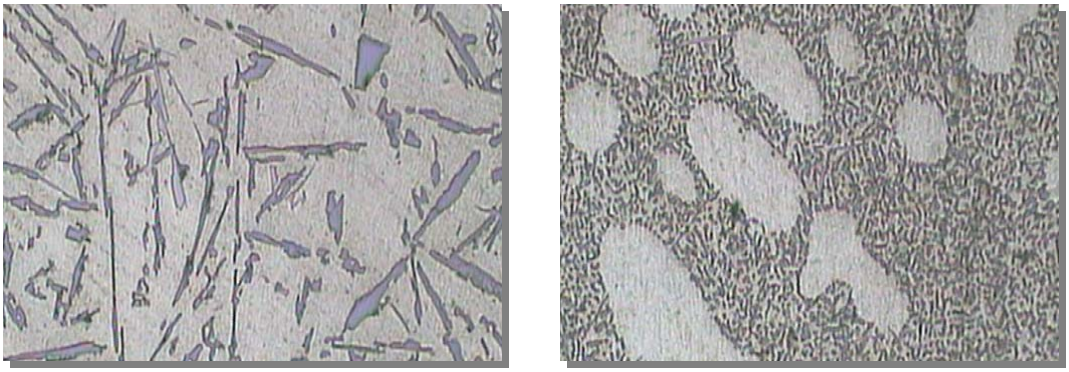

(a) (b)

Figure 4.1: Microstructure of LM6 alloy (a) Unmodified and (b) Strontium modified as-cast condition; etched 0.5% HF; X 200

Inspection under optical microscope had revealed the differences in microstructure of strontium modified and unmodified Al-Si alloy in as-cast conditions. It can be seen in Figure 4.1(a) that the matrix structure of unmodified alloy consists of α-aluminium dendrites with acicular eutectic silicon and plate shape primary silicon. The strontium treatment had produced remarkably fine distributed globular silicon as shown in Fig 4.1(b). It was also observed that the primary silicon crystals have been eliminated from the aluminum matrix. The results obtained are similar with findings reported by Haque and Kondic (1985); Emadi and Gruzleski (1995); Lu and Hellawell (1995).

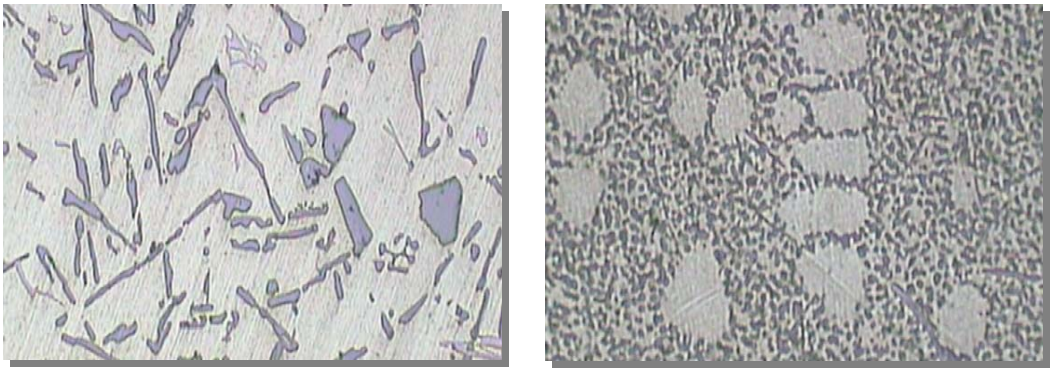

(a) (b)

Figure 4.2: Microstructure of LM6 alloy (a) Unmodified and (b) Strontium modified heat treated condition; etched 0.5% HF; X 200

On the other hand, in the heat treated specimen, shown in Figure 4.2(a), the eutectic silicon needles of the unmodified specimen display some spheroidizing and sharp corners have been rounded. The modified specimen in Figure 4.2(b) also has more uniform distribution and much finer structure of the silicon phase. Similar finding of thicky and less sharp structure was also obtained by Haque and Sharif (2001) in the modified alloy.

4.2.2 Effects of Modification on the Tensile Properties

The ultimate tensile strength (UTS) and percentage elongation have been carried out for both modified and unmodified alloys in as-cast and heat treated conditions. The results are graphically shown in Figures 4.3 (a) and (b).

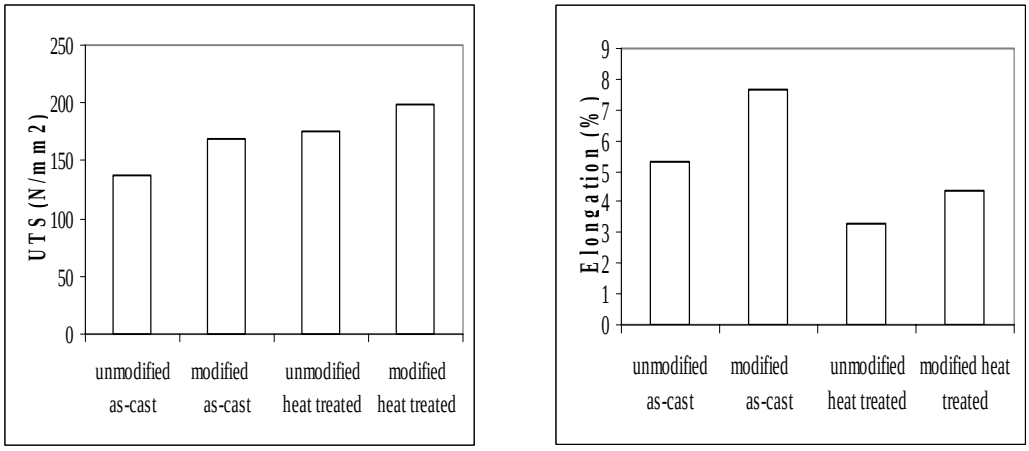

(a) (b)

Figure 4.3: (a) UTS and (b) Elongation for unmodified and modified LM6 alloy in the as-cast and heat treated condition

From above graphs, it is evident that heat treated alloys have better advantage in terms of strength. This is applicable for both unmodified and modified alloys. A higher tensile strength is suggested to be due to modification of the structure. Haque and Maleque (1998) and Dinnis, Otte, Kahle and Taylor (2004) have also reported that strontium modification results in a considerable improvement in tensile strength. Due to structural refinement, the tensile properties of the alloy have enhanced significantly.

It is also found that strontium modification improved the elongation. Similar observations were also reported by Emadi and Gruzleski, 1995; Shabel et al., 1995; Dinnis et al., 2004.

However, it is noticed that the strength in the heat treated specimen have increased at the expense of ductility. This is applicable for both unmodified and modified specimens.

4.2.3 Effects of Modification on the Hardness Properties

Hardness test was performed on the hardened steel disk and on the 5x5 mm wear test specimens. This is to ascertain that the disk will have a much higher ratio of hardness compared to the wear test specimens. The results have been graphically shown in Figure 4.4. It can be seen that the hardened steel disk is approximately 4.5 to 5.5 times harder than the unmodified and modified wear test specimens.

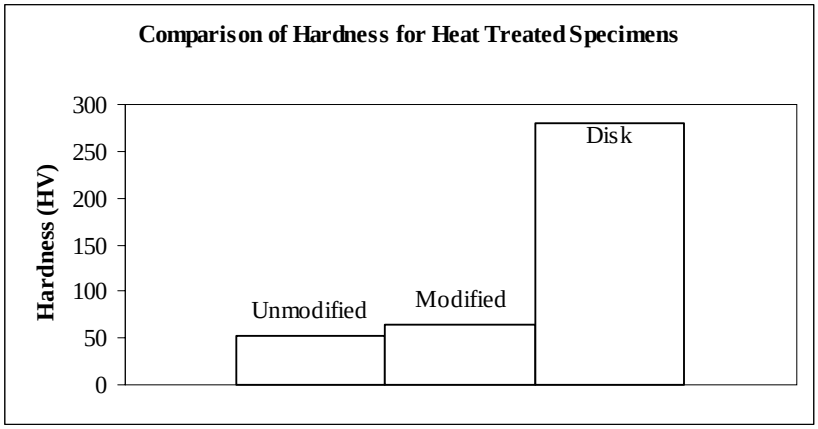

Figure 4.4: Comparison of hardness for hardened steel disk and heat treated specimens

In the figure, the hardness values of the heat treated test specimens as well as the hardened steel disk on which the actual wearing actions would be taken have been shown. The hardness value for modified Al-Si alloy specimens have increased about 1.5 times than the unmodified one. Combination of the silicon refinement and absence of primary silicon crystals in the microstructure contribute to accentuate the hardness property of the material. This is because in unmodified alloy, the large needle shaped silicon diminishes the mechanical properties by acting as crack initiator and stress rising site. Similar observations were also made by Lu and Hellawell, 1995.

Furthermore, the heat treatment was applied to the test samples produced rounded and less sharp silicon phase either primary or eutectic. This rounded shape reduces the tendency for crack initiation beginning at the sharp edges of the particles and increased strength and hardness properties. Similar observations were reported by Shabel et al., (1995).

4.3 WEAR TESTING

The wear experiments were carried out using pin-on-disc type of testing apparatus. The sliding contact wear tests used cylinder type of specimen on flat contact surface with lubricant. The investigation was carried out on the following aspects:

1. Comparison of wear rate between unmodified and modified LM6 alloy for both as-cast and heat treated conditions at following conditions:
    i. various rotational speeds,
    ii. various top loads,
    iii. various sliding distances,
2. Microscopic analysis of worn surfaces of the unmodified and modified LM6 alloy for both as-cast and heat treated conditions at following conditions:
    i. Constant speed, various load and sliding distance,
    ii. Constant load, various speed and sliding distance,
    iii. Constant sliding distance, various speed and load.

4.3.1 Wear Results for Speed Variables in As-Cast Condition

As the rotational speed of the hardened steel disk increases, the mass loss of the specimen material also increases. As the disk rotates, heat is generated between two contacting surfaces in sliding condition due to friction. This heat will reduce the surface energy of the material and since Al-Si eutectic alloy has less hardness compared to the hardened steel disk, the specimen will be abraded and adhered with the disk.

It can be seen from Figure 4.5 (a) that as the rotational speed of the hardened steel disk (counter body) is increased, the weight loss of unmodified as-cast specimens are also increasing whereas its modified counterpart is showing a declining trend. It may be due to refined structure of globular silicon produced from the modification treatment, which had improved the hardness property of the alloy.

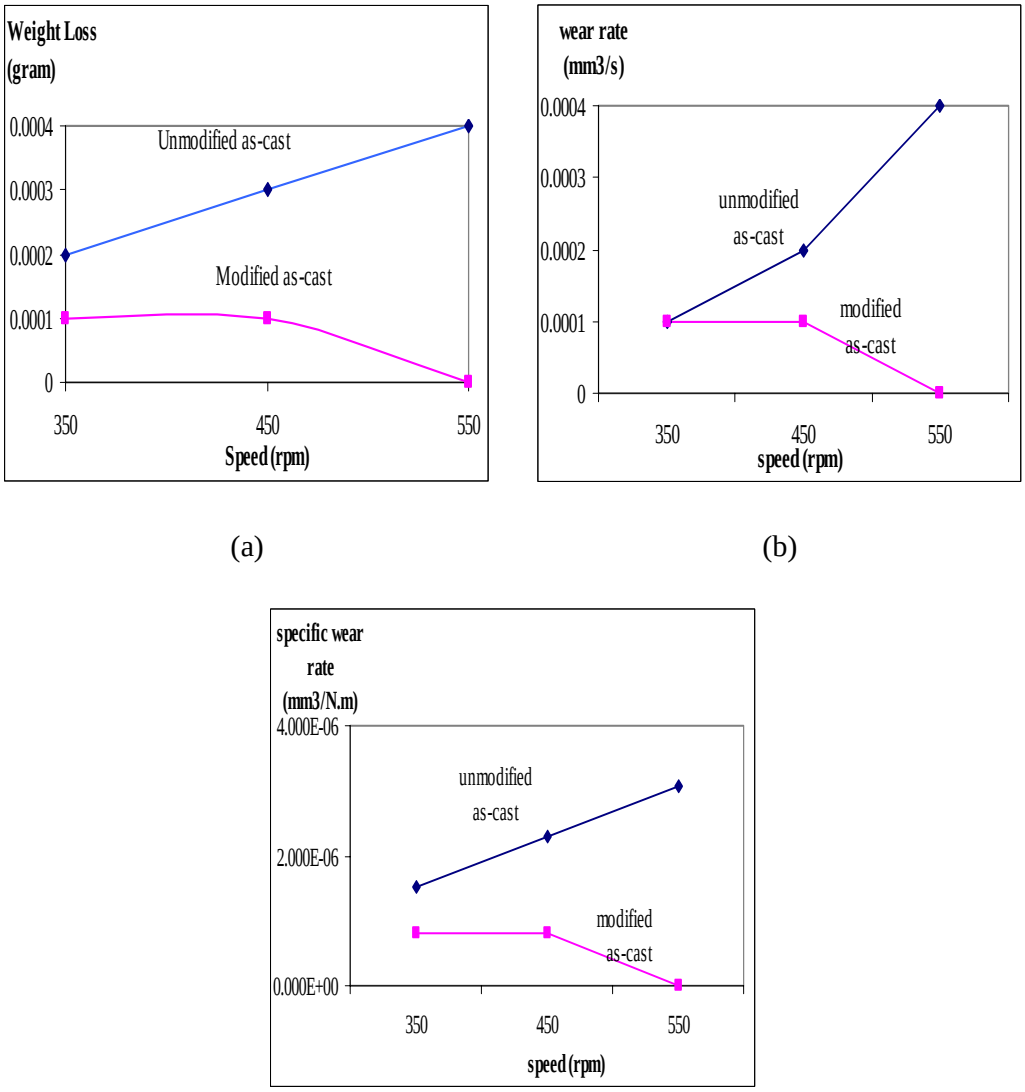

Figure 4.5: Wear results for unmodified and modified LM6 alloy in the as-cast condition with load 2.5 kg, sliding distance 2000 m and various speeds in terms of (a) weight loss (b) volumetric wear rate (c) specific wear rate

From Figures 4.5(b) and 4.5(c), it can be seen that both volumetric and specific wear rate display the same increasing pattern as the rotational speed is increased for unmodified as-cast specimen. Even in lubricated contact, there is still a significant rate of wear caused by the deformation sustained by the asperities and surface layers.

Modified as-cast specimen on the contrary, is showing a declining trend for both volumetric and specific wear rate. This demonstrates an improvement in wear properties of the modified specimens.

4.3.2 Worn Surfaces for Speed Variables in As-Cast Condition

From microscopic examination, unmodified as-cast in Figure 4.7 (a) display straight wear lines with small silicon particles. While the worn surface of modified as-cast specimen in Figure 4.8 (a) show an appearance of fibrous silicon. EDX analysis had confirmed that the fibrous element is indeed the refined silicon and the white flake like particle is also silicon as illustrated in Figure 4.6 below.

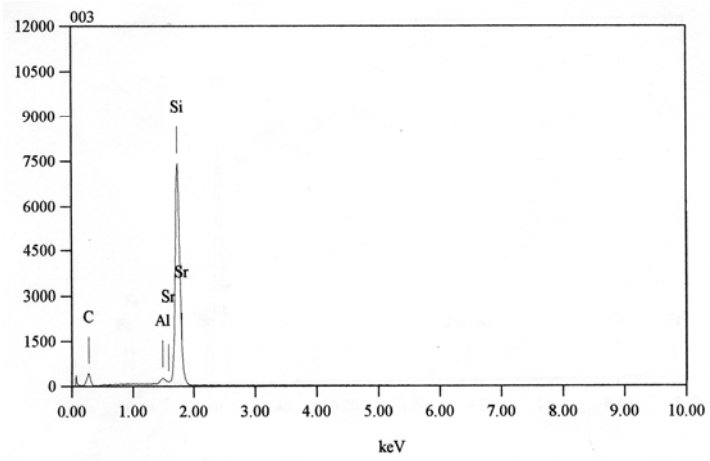

Figure 4.6: Qualification analysis using EDX to identify silicon element

When speed is increased from 350 to 450 rpm, the unmodified as-cast specimen shows deeper wear lines indicating that abrasive wear has occurred in Figure 4.7 (b). It is possible that as the sliding speed is increased, it has reduced the corrosivity of the lubricant, thus the chemical medium gives minimum weight loss. While the modified as-cast specimen shows an increase in the accumulation of fibrous silicon in Figure 4.8 (b). Finally, at the highest speed of 550 rpm, heat is developed

due to friction and caused the unmodified as-cast specimen of becoming softer and weaker. The critical difference between the effects of a temperature rise in the worn metal imposed by high grit speeds and changes in ambient temperature is that the grits remain relatively cool due to the transient nature of abrasion. Contact between a grit and the worn surface would be particularly short in the three-body abrasive wear mode, so that any heat generated in the deformed material would not diffuse into the grit. It is then possible that transient thermal softening occurs only in the deformed material while the grit remains virtually unaltered (Wing, 1989).

Perhaps this is why the worn surface of unmodified as-cast specimen in Figure 4.7 (c) is affected by local heating and deform plastically. The wear lines are also sharper and silicon particles are getting bigger. Whereas in Figure 4.8 (c) the modified as-cast specimen exhibits very high local stress that has caused surface fatigue. Despite surface deformation that has occurred, the mass loss is zero (Figure 4.5 (a)). Although no net change in weight or volume is recorded the phenomenon is still referred as wear. This is because the dimensional changes or roughening due to material transfer in the absence of measurable loss is considered as wear (Antler, 1981 and Bushan, 1999).

4.3.3 Wear Results for Speeds Variables in Heat Treated Condition

As for the heat treated samples, weight loss graph in Figure 4.9 (a) shows a declining trend for unmodified specimen. The modified specimen exhibits lower mass loss when the speed is at 350 rpm then decrease to a constant zero value when higher speed is applied. This may be due to the full heat treatment that has improved the hardness property of the specimens. In Figure 4.9 (b) the volumetric wear rate for the unmodified heat treated specimen indicates a slight increase as the speed is increased from 350 to 450 rpm. Whether lubricated or not, when two smooth bodies are sliding over each other, adhesive wear will take place and fragments are pulled off one surface and adhered to the other (Rabinowicz, 1995; Bushan, 1999).

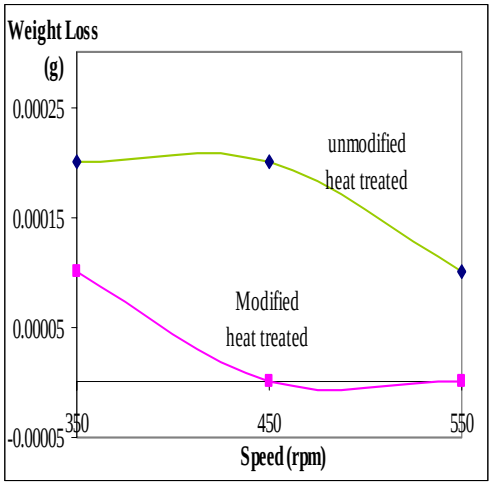

(a)

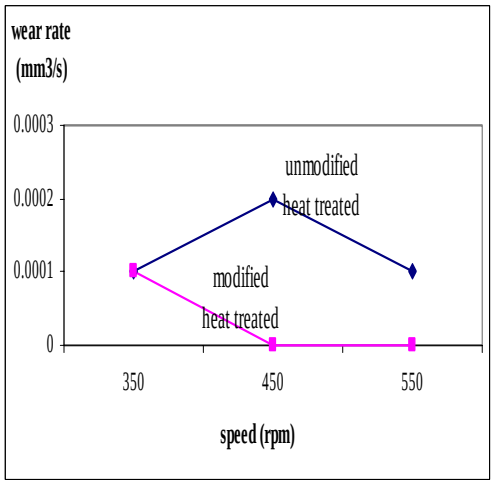

(b)

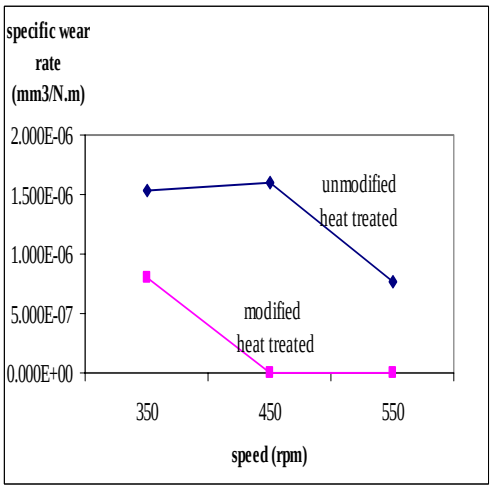

(c)

Figure 4.9 : Wear results for unmodified and modified LM6 alloy in the heat treated condition with load 2.5 kg, sliding distance 2000 m and various speeds in terms of (a) weight loss (b) volumetric wear rate (c) specific wear rate

However, the trend goes down as the speed is increased from 450 to 550 rpm. The modified heat treated specimen only gives a loss value when the speed is at 350 rpm. When the rotational speeds are at 450 rpm and 550 rpm, no measurable values

are shown. Specific wear rate in Figure 4.9 (c) for unmodified specimen displays a constant line at the beginning then drops to a lower value as the speed is increased to the maximum. Modified specimen in Figure 4.9 (c) exhibits a similar trend as found in volumetric wear rate graph for modified specimen. The lack of variation may be due to existence of zero values.

4.3.4 Worn Surfaces for Speed Variables in Heat Treated Condition

Figure 4.10(a) of unmodified heat treated specimen has few silicon particles and sharp scratches from abrasive wear. While Figure 4.11(a) has shallow scratches from adhesive wear and sparingly fibrous silicon on its surface. It is possibly chemical reaction between the worn material and corroding medium may have occured. The lubrication failure may lead to transition between corrosive and abrasive wear (Antler, 1981). As the speed is increased from 350 to 450 rpm, bigger sizes of silicon particles are accumulated on the worn surface of unmodified heat treated specimen in Figure 4.10(b), along with deeper wear lines. Its modified heat treated counterpart in Figure 4.11(b) only has few fibrous silicon with irregular scratches. At this point the mass loss is zero. Rabinowicz (1995) mentioned that the weighing technique had a limit of resolution around 10^{-4} g. There may be some measurable transfer or loss of material have occurred for this specimen but couldn't be detected by the weighing balance because the amount is less than 10^{-4} g, thus giving the zero value.

At the highest speed of 550 rpm, the weight loss of unmodified heat treated specimen is reduced. Repeated sliding action has worn out hard particles, which lead to some blunting of the hard asperities between the contacting surfaces. Figure 4.10(c) of unmodified heat treated specimen shows plastic deformation. Bigger silicon particles and broad wear lines are evident on the worn surface. However, the reduction in material removal may be due to clogging of the abrasive surface by abraded debris during wear. Heat localization has occurred due to friction at very high speed, in modified heat treated specimen which has maintained its hardness. As a result, it generated only mild fibrous silicon in Figure 4.11(c). This higher resistance performed by the modified heat treated specimens may be contributed by higher mechanical properties as compared to its unmodified counterparts.

CHAPTER 5

CONCLUSIONS AND RECOMMENDATIONS

5.1 CONCLUSIONS

Based on the experimental results and discussions of the previous chapters, the following major conclusions can be drawn from the present investigation:

1. Strontium modifies eutectic silicon in Al-Si alloys. Microstructural analysis and mechanical testing are two important tools that had conformed modification of the LM6 alloy was effectively performed.
2. The volume of material worn is not absolutely proportional to the rotational speed, load, and sliding distance. When higher rotational speed, load, and sliding distance were applied, the volume of material worn was found to be decreased.
3. The volume of material worn is inversely proportional to the hardness of the material.
4. Transitional behaviour is exhibited between adhesive wear, abrasive wear, corrosive wear and surface fatigue in the wear study of the unmodified Al-Si alloys. On the other hand, surface fatigue wear is dominating the wear damage in strontium modified Al-Si alloy, affected by transition between other modes of wear.
5. During wear, measurable material/debris transfer could occur resulting in weight gain of the sliding specimen. This is due to accumulation of the material on the surface.

6. Combination of modification and heat treatment when applied to Al-Si eutectic alloy has shown better resistance towards wear. Thus it is recommended for industrial applications.

5.2 RECOMMENDATIONS FOR FUTURE WORKS

There are a few aspects of the present study which may be carried out in future, they are listed below;

1. The effect of strontium modification on wear behaviours was investigated in this study using a pin-on-disc type of wear experiment. It is suggested to perform the experiments with other contact geometry models so that comparison can be made to identify the best method.
2. Although the effect of strontium on wear behaviours was investigated under lubricant sliding condition, it would be useful to incorporate other parameters of the lubricant used such as viscosity of the liquid, or the temperature range of specific engine oil, etc.
3. The investigation was performed using sole modifier only. It would be interesting to investigate the interaction of strontium with other modifiers, and to discover how they would affect wear properties of LM6 alloy.
4. The effect of strontium was investigated with LM6 alloy in this study. It would be useful to carry out the experiments for other Al-Si foundry alloys.

BIBLIOGRAPHY

Aluminum strontium master alloy. (2004). Retrieved November 12, 2005.

Antler, M. (1981, March). Sliding wear of metallic contacts, *IEEE Trans. CHMT-4*, (1), 15-16.

Apelian, D., Sigworth, G.K., & Whaler, K.R. (1984). Assessment of grain refinement and modification of Al-Si foundry alloys by thermal analysis, *Trans. of AFS. 92*, 297-307.

Archard, J.F., & Hirst, W. (1956). The wear of metals under unlubricated conditions, Paper presented at the Proc. Roy. Soc.A236.

Arnell, R.D., Davies, P.B., Halling J., & Whomes, T.L. (1991). *Tribology: Principles and design applications.* London: Macmillan, 2-10.

Bayer, R.G. (1995). *Wear testing*, vol. 8, Mechanical Testing, ASM Handbook,: 600, 604-607.

Bowden, F.B., & Rowe, G.W. (1956). The adhesion of clean metals. Paper presented at the Proc. Royal Soc., London.

Bowden, F.P., & Tabor, D. (1964). *The friction and lubrication of solids.* (part 2), Oxford University Press.

Braiman, Y., Cummings, P., & Granick, S. (2004). Frontiers in tribology at the atomic scale and nano scales, white paper prepared in workshop at ORNL. Retrieved January 20, 2006.

Buckley, D.H. (1981). *Surface effects in adhesion, friction, wear and lubrication.* Amsterdam: Elsevier.

Bushan, B. (1999). Principles and applications of tribology. New York: John Wiley & Sons.: 3-8, 100-109, 509-511, 494-507, 480-490

Challen, J.M., McLean, L.J., & Oxley, P.L.B. (1984). Plastic deformation of a metal surface in sliding contact with a hard wedge: its relation to friction and wear. Paper presented at the Proc. Roy. Soc.,London.

Christ, B.W. (1985). *Effect of specimen preparation, setup and test procedure on test results* (desk edn.). Metals Handbook, ASM: 28-30.

Closset, B., & Gruzleski, J.E. (1982). Structure and properties of hypoeutectic Al-Si-Mg alloys modification with pure strontium, *Metallurgical Trans. A, 13A*, 945.

Cornell, R., & Bhadeshia, H. (2002, July). *Aluminum silicon alloys.* Retrieved November 10, 2005.

Davis, J.R., Davis & Associates. (1986). *Friction and wear of internal combustion engine parts.* (3rd print). Aluminum & Aluminum Alloys, The Material Information Society, ASM Specialty Handbook: 553-560.

Dieter, G.E. (1985). *Tension and compression testing* (desk edn.). Metals Handbook, ASM: 12-15.

Dinnis, C.M., Otte, M.O., Dahle, A.K., & Taylor, J.A. (2004, November). The influence of strontium on porosity formation in Al-Si alloys, *Metallurgical and Materials Transactions A, 35*, 3531.

Ejiofor, J.U., & Reddy, R.G. (1997). Developments in the processing and properties of particulate Al-Si composites, *JOM, The Minerals, Metals and Materials Society 49* (11) 1997, 31-37.

Emadi, D., & Gruzleski, J.E. (1995, March). Combating Al-Si porosity: The strontium hydrogen myth, *Modern Casting.*

Engine filtration and maintenance. (2003). Retrieved December 20, 2004.

Eyre, T.S. (1991). Universal wear machine operations manual, England: Biceri Ltd.

George, F.V.V, Research & technology buehler guide complete, 2002, USA.

Gruzleski, J.E., & Closset, B. (1990). The treatment of liquid Al-Si alloy, *Trans. of AFS*,: chapters 3,9,13.

Gruzleski, J.E., Paray, F., Shabestari, S.G., & Mulazimoglu, M.H. (1995). Applications of strontium in cast and wrought aluminum alloy, recent metallurgical advances in light metals industries: 341.

Haque, M.M., & Ahmad Faris Ismail (2005). Effect of superheating temperatures on microstructure and properties of strontium modified aluminum-silicon alloy, *Journal of Materials Processing Technology, 162-163*, 312-316.

Haque, M.M., & Kondic, V. (1985). Influence of strontium on solidifation of aluminum-silicon alloys, Proc. on Light Metals: Science & Tech.: Switzerland.

Haque, M.M., & Sharif, A. (2001). Study on wear properties of aluminum-silicon piston alloy. *J. of Materials Processing Technology,* 118, 69-73.

Haque, M.M., & Maleque, M.A. (1998). Effect of process variables on structure and properties of alunium–silicon piston alloy, *Journal of Materials Processing Technology 77*,122-128.

Haque, M.M. (1983). Factors affecting strontium modification, Metals Forum, Australia.

Heat treating of aluminum alloy (1995), vol. 1.4, ASM Handbook: 841-879.

Kaufman, J.G. (2000). *Introduction to aluminum alloys and tempers.* ASM International: 36-37, 81-82, 92-93.

Kayaba, T., & Kato, K. (1979). The analysis of adhesive wear mechanism by successive observations of the wear process in SEM. Ludema, K.C., W.A Glaeser W.A., & Rhee, S.K. (eds.), New York: Publ. American Society of Mechanical Engineers, 45-47.

Kayaba, T. (1984). The latest investigation of wear by the microscopic observations, *JSLE Trans. 29*, 9-14.

Khruschov, M.M., & Babichev, M.A. (1956). Trenie i iznos v mash [Investigation of the wear of metals and alloys by rubbing on abrasive surface, friction and wear in machines]., Moscow: Acad. Sci. USSR, pp. 351-358.

Khruschov, M.M. (1967). Resistance of metal to wear by abrasion as related to hardness, Proc. Conf. on Lubrication and Wear, Inst. Mech. Engrs., Publ., London, pp. 635-639.

Konivopoulus, K., Saka, N., & Suh, N.P. (1985). The mechanism of friction in boundary lubrication, *Trans. ASME, J. of Tribology. 107*, 452-453.

Lu, S., & Hellawell (1995, February). Modification of Al-Si alloys: Modification, thermal analysis and mechanisms. *J. of Metals:* 38-40.

Lyman, T. (1961). Metals handbook (8^{th} edtn.). vol. 1, American Society for Metals: 250-251.

Parker, S.P. (1982). *McGaw-Hill Encyclopedia of Science& Technology.* (p 545) McGraw-Hill.

Rabinowicz, E. (1995). *Friction & wear of materials* (2^{nd} edn.). New York: John Wiley & Sons.: 143-149, 211-214, 218.

Rao, P.N. (2001). *Manufacturing technology; foundry, forming and welding* (2^{nd} edtn.), Singapore: McGraw Hill Int.: 61-65.

Rengstorff, G.W., Miyoshi, K., & Buckley, D.H. (1986). Interaction of sulfuric acid corrosion & mechanical wear of iron. *ASLE Trans. 29,* 43-44.

Richardson, R.C.D. (1967). The abrasive wear of metals and alloys. Paper presented at the Proc. Inst. Mech. Engrs. Pt. 3A.

Rigney, D.A., & Hirth, J.P. (1979). Plastic deformation and sliding friction of metals. *Wear 53*, 370.

Shabel, B.S., Granger, D.A., & Truckner, W.G. (1995). *Friction and wear of aluminum- silicon alloy*. vol. 18, ASM Handbook: 785.

Sigworth, G.K. (1983). Theoretical & practical aspects of the modification of Al-Si alloys, *Trans. of AFS. 91*, 7-16.

Stachowiak, G.W., & Batchelor, A.W. (1993) *Engineering tribology*. Amsterdam: Elsevier: 535-550, 613-631, 638-645, 658-660, 557-574.

Taylor, I. (2002, February). Car lubricants: fact and friction. *Physics World*, IOP Publishing Ltd.: p. 39.

Ting, L.L. (1980). *Lubricated piston rings and cylinder bore wear*. Wear Control Handbook, American Society of Mechanical Engineers: 609-611.

Tsujimiura, T., & Kikawa T. (1998). *Tribology in railway*. QR Sep., vol. 39, No. 3.

Tuti Yasmin Alias, Khalid, A.A., & Haque, M.M. (2004). Tribological properties of aluminum-silicon eutectic base alloy under dry sliding condition, *Journal of Materials Processing Technology, 153-154*, 833-838.

Vingsbo, O. (1979). Wear and wear mechanisms. Ludema, K.C., W.A Glaeser W.A., & Rhee, S.K. (eds.), New York: Publ. American Society of Mechanical Engineers, 620-621.

Wing, N. (1989). The transformation of soft-abrasive wear into hard abrasive wear under the effect of frictional heat, *Tribology Trans. 32*, 85.

http://www.aleastur.com

http://www.csm.ornl.gov/meetings/FITAS

http://www.msm.cam.ac.uk/phase-trans/abstract/m7-8.html

http//:www.amsoil.com/engine.html

APPENDIX A

SAMPLE CALCULATION FOR VOLUMETRIC WEAR RATE AND SPECIFIC WEAR RATE

By using densitimeter mass in air of the sample, m_a and in water,m_w were measured and recorded. To find the density of the sample, the following formula was used;

$$\rho = \frac{m_a}{m_a - m_w} X \rho_w$$

$$m_a = 15.91 g$$
$$m_w = 9.93 g$$

Where ρ_w is the density of water.
The density for aluminum silicon eutectic alloy was found out as;

$$\rho = \frac{15.91 g}{15.91 g - 9.93 g} X 1 \, {}^{g}\!/_{cm^3}$$

$$\rho = 2.66 \, {}^{g}\!/_{cm^3}$$

$$\rho = 2.66 X 10^{-3} \, {}^{g}\!/_{mm^3}$$

Volume loss, W was calculated using the following formula;

$$W = \frac{\Delta m}{\rho}$$

Where Δm is the mass loss of specimen due to wear.

$$W = \frac{0.0032 g}{2.66 X 10^{-3} \, {}^{g}\!/_{mm^3}}$$

$$W = 1.203 mm^3$$

Thus, the wear rate is as follows;

$$W(t) = \frac{W}{t} = \frac{1.203 mm^3}{(9.23 X\, 60) s}$$
$$= 0.0022\, mm^3 / s$$

Where ***t*** is time in seconds.

Therefore, the specific wear rate W_s for specimen is calculated by using the following formula;

$$W_s = \frac{W(t)}{v_s F_n}$$

Where v_s is sliding velocity in **m/*s*** and F_n is applied normal load in **N** or **kgm/s^2**.

$$v_s = N \pi D_{\exp}$$
$$= (300 rpm)(3.142)(2 X\, 65 mm)$$
$$= 122538\, mm / \min X \frac{1 \min}{60 s} X \frac{1 m}{1000 mm}$$
$$= 2.0423\, m / s$$

Then, the specific wear rate was found out as

$$W_s = \frac{W(t)}{v_s F_n}$$
$$= \frac{0.0022\, mm^3 / s}{(2.0423\, m / s)(1.25 kg)(9.81\, m / s^2)}$$
$$= 8.675 X 10^{-5}\, mm^3 / N.m$$

APPENDIX B

SAMPLE CALCULATION FOR VOLUME OF AL-SI ALLOY REQUIRED FOR UNMODIFIED SPECIMEN, MODIFIED SPECIMEN, AND METAL CRUCIBLE

Calculation for unmodified specimen

volume for cylinder is $\pi r^2 h$
where $\pi = 3.142$, r is the radius and h is the height
$v_1 = \pi(1cm)^2(7cm) \therefore v_1 = 21.99cm^3$
Since $v_1 = v_3$, $\therefore v_3 = 21.99cm^3$
$v_2 = \pi(0.5cm)^2(6cm)$,
$\therefore v_2 = 4.71cm^3$
So, the total volume would be $v_1 + v_2 + v_3 = v_{unmodified}$ = 48.69 cm^3
From formula, mass(m) = volume (v) × density (ρ)
It is known that density of aluminum is $2.7 \, g/cm^3$
So, $mass(m) = 48.69cm^3 \times 2.7 \, g/cm^3$
$= 131.46g$
Tolerance for the mould is given at 50% from the mass, which will be 65 grams
So, the weight of aluminum to be melt is $mass(m)$ + tolerance
$\therefore 131.46g + 65.73g = 197.19g$
Total weight of aluminium alloy to be melt is 197 g ≈ 200 g
This approximation is only for one specimen. For the purpose of the research, four tensile specimens will be cast, therefore approximately 1 kg of aluminum alloy is to be melt in the furnace.

Calculation for modified specimen with 0.1% of strontium

1000 grams from LM6 alloy will be added with 0.1% of strontium from the master alloy consists of 90% Al-10% Sr
So, 1000 g of LM6---------- $\frac{0.1 \times 1000g}{100} = 1.0g$
However, as the master alloy is consisted of 90%Al-10% Sr, therefore 10 grams of the master alloy is required.

Calculation for volume of aluminum that can be contained by the metal crucible

volume for cylinder is $\pi r^2 h$
where $\pi = 3.142$, r is the radius and h is the height
Hence, $\pi(4cm)^2(12cm) = 603.19\ \text{cm}^3$
From formula, volume of crucible (v_c) $\times$ density (ρ) = mass of crucible (m)
It is known that density of aluminum is $2.7\ g/cm^3$
$\therefore$ mass (m) = 603.19 cm^3 x $2.7\ g/cm^3$

$= 1.63 \times 10^3\ \text{g}$

It is known that $1000g < 1.63 \times 10^3 g$
So, it can be concluded that the crucible is able to contain the amount of molten aluminum alloy.

APPENDIX C

SURFACE ROUGHNESS MEASUREMENT

The surface measurements were taken for the hardened steel disk and all wear specimens to ensure that values are within the acceptable range. All final results were averaged from five readings. The results are incorporated in Table C

Table C
Average surface roughness of disk and specimen for each set of wear experiment using different variables

Conditions		Average Surface Roughnes, Ra (μm)	
		Hardened steel disk	Wear Specimen
Unmodified as-cast	Speed variables are 350, 450 and 550 rpm, keeping load constant at 2.5 kg and distance constant at 2000m	0.5167	0.3534
	Load variables are 1.5, 2.5 and 3.5 kg, keeping speed constant at 450 rpm and sliding distance constant at 2000m	0.5067	0.3300
	Sliding distance variables are 1500, 2000 and 2500 m, keeping sped constant at 450 rpm and load constant at 2.5 kg	0.5934	0.2967
Modified as-cast	Speed variables are 350, 450 and 550 rpm, keeping load constant at 2.5 kg and distance constant at 2000m	0.4867	0.5034
	Load variables are 1.5, 2.5 and 3.5 kg, keeping speed constant at 450 rpm and sliding distance constant at 2000m	0.5067	0.5434
	Sliding distance variables are 1500, 2000 and 2500 m, keeping sped constant at 450 rpm and load constant at 2.5 kg	0.5067	0.5934
Unmodified heat treated	Speed variables are 350, 450 and 550 rpm, keeping load constant at 2.5 kg and distance constant at 2000m	0.4967	0.3167

	Load variables are 1.5, 2.5 and 3.5 kg, keeping speed constant at 450 rpm and sliding distance constant at 2000m	0.4867	0.3800
	Sliding distance variables are 1500, 2000 and 2500 m, keeping sped constant at 450 rpm and load constant at 2.5 kg	0.5134	0.4000
Modified heat treated	Speed variables are 350, 450 and 550 rpm, keeping load constant at 2.5 kg and distance constant at 2000m	0.5067	0.5734
	Load variables are 1.5, 2.5 and 3.5 kg, keeping speed constant at 450 rpm and sliding distance constant at 2000m	0.4967	0.5000
	Sliding distance variables are 1500, 2000 and 2500 m, keeping sped constant at 450 rpm and load constant at 2.5 kg	0.5900	0.6034

APPENDIX D

SAMPLE CALCULATION FOR ULTIMATE TENSILE STRENGTH AND ELONGATION FROM TENSILE TEST

Table D
Data from tensile test

Specimen	Condition	Initial diameter, D_o (mm)	Initial gauge length, L_o(mm)	Final gauge length, L_f (mm)	Percentage of elongation (%)	Ultimate tensile stress, UTS (N/mm^2)	Maximum Force (kN)
Unmodified	As cast	12.79	50	52.21	4.42	137.07	17.61
		12.56	50	52.33	4.66	135.66	16.82
Modified	As cast	12.37	50	53.82	7.64	166.67	20.03
		12.25	50	53.71	7.42	168.51	19.86
Unmodified	Heat treated	13.14	50	51.48	2.96	174.18	23.62
		13.31	50	51.64	3.28	176.01	24.49
Modified	Heat treated	12.99	50	52.09	4.18	197.16	26.13
		12.72	50	52.17	4.34	198.46	25.22

Calculation for: 1) UTS = F/A_o

2) Percentage of Elongation = $\frac{L_f - L_o}{L_o} \times 100$

There are two specimens for each parameter calculated.

<u>LM6 (as cast)</u>

1) UTS = F/A_o

$= \frac{16.82 \times 10^3}{123.99}$

$= 135.66\ N/mm^2$

when F = 16.82 kN

$A_o = \frac{\pi}{4}(D_o)^2$

$A_o = \frac{\pi}{4}(12.56)^2 = 123.99\ mm^2$

1) % of Elongation = $\frac{L_f - L_o}{L_o} \times 100$

$= \frac{52.21 - 50}{50} \times 100$

$= 4.42\ \%$

2) UTS = F/A_o $= \frac{17.61\times10^3}{128.48}$ = 137.07 N/mm^2 when F = 17.61 kN $A_o = \frac{\pi}{4}(D_o)^2$ $A_o = \frac{\pi}{4}(12.79)^2$ = 128.48 mm^2	2) % of Elongation = $\frac{L_f - L_o}{L_o}\times100$ $= \frac{52.17-50}{50}\times100$ = 4.34 %

LM6 + 0.1 % Sr (as cast)

1) UTS = F/A_o $= \frac{19.86\times10^3}{117.86}$ = 160.12 N/mm^2 when F = 19.86 kN $A_o = \frac{\pi}{4}(D_o)^2$ $= \frac{\pi}{4}(12.25)^2$ = 117.86 mm^2	1) % of Elongation = $\frac{L_f - L_o}{L_o}\times100$ $= \frac{53.82-50}{50}\times100$ = 7.64 %
2) UTS = F/A_o $= \frac{20.03\times10^3}{120.18}$ = 166.67 N/mm^2 when F = 20.03 kN $A_o = \frac{\pi}{4}(D_o)^2$ $= \frac{\pi}{4}(12.37)^2$ = 120.18 mm^2	2) % of Elongation = $\frac{L_f - L_o}{L_o}\times100$ $= \frac{53.71-50}{50}\times100$ = 7.42 %

LM6 (heat treated)

1) UTS = F/A_o $= \frac{23.62 \times 10^3}{135.61}$ = 174.18 N/mm^2 when F = 23.62 kN $A_o = \frac{\pi}{4}(D_o)^2$ $= \frac{\pi}{4}(13.14)^2$ = 135.61 mm^2	1) % of Elongation = $\frac{L_f - L_o}{L_o} \times 100$ $= \frac{51.64 - 50}{50} \times 100$ = 3.28 %
2) UTS = F/A_o $= \frac{24.49 \times 10^3}{139.14}$ = 176.01 N/mm^2 when F = 24.49 kN $A_o = \frac{\pi}{4}(D_o)^2$ $= \frac{\pi}{4}(13.31)^2$ = 139.14 mm^2	2) % of Elongation = $\frac{L_f - L_o}{L_o} \times 100$ $= \frac{51.48 - 50}{50} \times 100$ = 2.96 %

LM6 + 0.1 % Sr (heat treated)

1) UTS = F/A_o $= \frac{26.13 \times 10^3}{132.53}$ = 197.16 N/mm^2 when F = 26.13 kN $A_o = \frac{\pi}{4}(D_o)^2$ $= \frac{\pi}{4}(12.99)^2$ = 132.53 mm^2	1) % of Elongation = $\frac{L_f - L_o}{L_o} \times 100$ $= \frac{52.09 - 50}{50} \times 100$ = 4.18 %

2) UTS $= F/A_o$ $= \frac{25.22 \times 10^3}{127.08}$ $= 198.46$ N/mm^2 when F = 25.22 kN $A_o = \frac{\pi}{4}(D_o)^2$ $= \frac{\pi}{4}(12.72)^2 = 127.08$ mm^2	2) % of Elongation $= \frac{L_f - L_o}{L_o} \times 100$ $= \frac{52.17 - 50}{50} \times 100$ $= 4.34\%$

APPENDIX E

WEAR RESULTS

Table 1E
Weight loss for unmodified and modified LM6 alloy in the as-cast condition using speed variables (load 2.5 kg and sliding distance 2000 m)

Speed (rpm)	Weight Loss(gram)	
	unmodified as cast	modified as cast
350	0.0002	0.0001
450	0.0003	0.0001
550	0.0004	0.0000

Table 2E
Weight loss for unmodified and modified LM6 alloy in the as-cast condition using load variables (speed 450 rpm and sliding distance 2000 m)

Input weight (kg)	Weight Loss(grams)	
	unmodified as cast	modified as cast
1.5	0.0002	0.0001
2.5	0.0003	0.0001
3.5	0.0001	0.0000

Table 3E
Weight loss for unmodified and modified LM6 alloy in the as-cast condition using sliding distance variables (speed 450 rpm and load 2.5 kg)

Sliding Distances (m)	Weight Loss (grams)	
	Unmodified as-cast	Modified as-cast
1500	0.0002	0.0001
2000	0.0003	0.0001
2500	0.0003	-0.0001

Table 4E
Weight loss for unmodified and modified LM6 alloy in the heat treated condition using speed variables (load 2.5 kg and sliding distance 2000 m)

Speed (rpm)	Weight Loss (grams)	
	Unmodified heat treated	Modified heat treated
350	0.0002	0.0001
450	0.0002	0.0000
550	0.0001	0.0000

Table 5E
Weight loss for unmodified and modified LM6 alloy in the heat treated condition using load variables (speed 450 rpm and sliding distance 2000 m)

Load (kg)	Weight Loss (grams)	
	Unmodified heat treated	Modified heat treated
1.5	0.0001	0.0001
2.5	0.0002	0.0000
3.5	0.0001	0.0000

Table 6E
Weight loss for unmodified and modified LM6 alloy in the heat treated condition using sliding distance variables (speed 450 rpm and load 2.5 kg)

Sliding Distance (m)	Weight Loss (grams)	
	Unmodified heat treated	Modified heat treated
1500	0.0001	0.0001
2000	0.0002	0.0000
2500	0.0002	0.0000

Table 7E
Wear rate for unmodified and modified LM6 alloy in the as-cast condition using speed variables (load 2.5 kg and sliding distance 2000 m)

Speed (rpm)	Wear rate (mm^3/s)	
	Unmodified as-cast	Modified as-cast
350	0.0001	0.0001
450	0.0002	0.0001
550	0.0004	0.0000

Table 8E
Wear rate for unmodified and modified LM6 alloy in the as-cast condition using load variables (speed 450 rpm and sliding distance 2000 m)

Load (kg)	Wear rate (mm^3/s)	
	Unmodified as-cast	Modified as-cast
1.5	0.0001	0.0001
2.5	0.0002	0.0001
3.5	0.0001	0.0000

Table 9E
Wear rate for unmodified and modified LM6 alloy in the as-cast condition using sliding distance variables (speed 450 rpm and load 2.5 kg)

Sliding distance (m)	Wear rate (mm^3/s)	
	Unmodified as-cast	Modified as-cast
1500	0.0002	0.0001
2000	0.0002	0.0001
2500	0.0001	-0.0001

Table 10E
Wear rate for unmodified and modified LM6 alloy in the heat treated condition using speed variables (load 2.5 kg and sliding distance 2000 m)

Speed (rpm)	Wear rate (mm^3/s)	
	Unmodified heat treated	Modified heat treated
350	0.0001	0.0001
450	0.0002	0.0000
550	0.0001	0.0000

Table 11E
Wear rate for unmodified and modified LM6 alloy in the heat treated condition using load variables (speed 450 rpm and sliding distance 2000 m)

Load (kg)	Wear rate (mm^3/s)	
	Unmodified heat treated	Modified heat treated
1.5	0.0001	0.0001
2.5	0.0002	0.0000
3.5	0.0001	0.0000

Table 12E
Wear rate for unmodified and modified LM6 alloy in the heat treated condition using sliding distance variables (speed 450 rpm and load 2.5 kg)

Sliding distances (m)	Wear rate (mm^3/s)	
	Unmodified heat treated	Modified heat treated
1500	0.0001	0.0001
2000	0.0002	0.0000
2500	0.0001	0.0000

Table 13E
Specific wear rate for unmodified and modified LM6 alloy in the as-cast condition using speed variables (load 2.5 kg and sliding distance 2000 m)

Speed (rpm)	Specific wear rate (mm^3/N.m)	
	Unmodified as-cast	Modified as-cast
350	1.5337E-06	7.9938E-07
450	2.2977E-06	7.9991E-07
550	3.0652E-06	0.0000E+00

Table 14E
Specific wear rate for unmodified and modified LM6 alloy in the as-cast condition using load variables (speed 450 rpm and sliding distance 2000 m)

Load (kg)	Specific wear rate (mm^3/N.m)	
	Unmodified as-cast	Modified as-cast
1.5	1.2777E-06	1.3318E-06
2.5	2.2977E-06	7.9991E-07
3.5	5.4742E-07	0.0000E+00

Table 15E
Specific wear rate for unmodified and modified LM6 alloy in the as-cast condition using sliding distance variables (speed 450 rpm and load 2.5 kg)

Sliding distance (m)	Specific wear rate (mm^3/N.m)	
	Unmodified as-cast	Modified as-cast
1500	2.0443E-06	1.0655E-06
2000	2.2977E-06	7.9991E-07
2500	1.8390E-06	-6.3974E-07

Table 16E
Specific wear rate for unmodified and modified LM6 alloy in the heat treated condition using speed variables (load 2.5 kg and sliding distance 2000 m)

Speed (rpm)	Specific wear rate (mm^3/N.m)	
	Unmodified heat treated	Modified heat treated
350	1.5326E-06	7.9925E-07
450	1.5936E-06	0.0000E+00
550	7.6690E-07	0.0000E+00

Table 17E
Specific wear rate for unmodified and modified LM6 alloy in the heat treated condition using load variables (speed 450 rpm and sliding distance 2000 m)

Load (kg)	Specific wear rate (mm^3/N.m)	
	Unmodified heat treated	Modified heat treated
1.5	1.2777E-06	1.3328E-06
2.5	1.5936E-06	0.0000E+00
3.5	5.4742E-07	0.0000E+00

Table 18E
Specific wear rate for unmodified and modified LM6 alloy in the heat treated condition using sliding distance variables (speed 450 rpm and load 2.5 kg)

Sliding distance (m)	Specific wear rate (mm^3/N.m)	
	Unmodified heat treated	Modified heat treated
1500	1.0221E-06	1.0655E-06
2000	1.5936E-06	0.0000E+00
2500	1.2264E-06	0.0000E+00